• U C •

FCTUC FACULDADE DE CIÊNCIAS
E TECNOLOGIA
UNIVERSIDADE DE COIMBRA

Henrique Jorge de Figueiredo Tavares Batista

Development of nanofibrous membranes for localized and controlled release of antibiotics

Dissertação apresentada à Universidade de Coimbra para cumprimento dos requisitos necessários à obtenção do grau de Mestre em Engenharia Biomédica

Supervisors:

Prof. Drª. Margarida Figueiredo

Drª. Patrícia Coimbra

Coimbra, 2015

This work was developed in collaboration with:

Departamento de Engenharia Química

Acknowledgements

Em primeiro lugar quero agradecer à Dr[a] Patrícia Coimbra por todo o apoio e dedicação que deu a este trabalho, e por uma orientação fenomenal. Sem dúvida que este trabalho não teria sido possível sem o papel incansável que desempenhou no decorrer deste projecto. Agradeço também à Prof. Dr[a] Margarida Figueiredo pela disponibilidade para ser minha orientadora e pela oportunidade de trabalhar neste projecto.

Quero também agradecer ao Prof. Dr. Filipe Antunes e ao Prof. Dr. João Moreira pela disponibilidade e interesse que demonstraram ao constituírem o júri que avaliou esta dissertação. Agradeço-lhes também por me terem ajudado no sentido da entrega da tese, quando com todo o direito me podiam ter recusado.

Aos meus pais, à minha irmã e à minha avó, pelo apoio, carinho e acompanhamento que, cada um à sua maneira, me deram algumas vezes mesmo sem se aperceberem. Por me porem no caminho certo quando me desviei e por acreditarem sempre em mim, mesmo quando eu próprio não acreditei.

À Carolina, um agradecimento muito especial, por todo o amor, compreensão e muita paciência que me deu ao longo de 3 anos, e especialmente ao longo destes últimos meses. Por sempre estar do meu lado nos momentos felizes, e também nos momentos menos felizes.

Aos meus amigos. Ao Nuno Cantão e Francisco Almeida, pelas gargalhadas, pelos desesperos electrónicos, pela procrastinação e pelo convívio. Ao Vicente, David e Pedro, também pelas gargalhadas, pelos desvios e pelos momentos de insanidade completa (no bom sentido). Tudo são momentos e amizades que ficam para a vida.

Abstract

The objective of this work is to develop polymer nanofibrous membranes capable of localized and controlled release of the Gentamicin Sulfate (GS) antibiotic. It is intended that these systems may be implanted during orthopedic surgery, in order to prevent or treat the possible development of bone infection in the post-surgery period.

The main objective behind localized controlled release of drugs is to develop drug delivery systems that have the ability to control the concentration of a drug available in the organism in space and time. Most of the developed systems of this kind have a polymer base, which is due to the variety of chemical, physical and biological properties exhibited by these materials, as well as their ease of production. One method for the processing of polymers that is considered attractive for the development of drug delivery systems is electrospinning, a technique that allows for the production of polymer fibers with diameters from a few micrometers to hundreds of nanometers. These structures present a high surface area to volume ratio, which is favorable for the incorporation and release of drugs. On the other hand this characteristic also favors a fast and extensive release of the incorporated drug, which might be undesirable for certain types of therapy. This problem is exacerbated when the drug to be incorporated is hydrophilic, as is the case for Gentamicin Sulfate. One possible solution for this problem comes in the shape of mesoporous silica nanoparticles (MSN's), a much investigated material for immobilization and release of drugs.

Therefore, in an attempt to obtain a more controlled release of GS over a relatively long period of time, in this work GS was immobilized in MSN's. These particles were then dispersed in a polymer solution which was later electrospun, resulting in the incorporation of GS loaded MSN in the electrospun fibers. The polymer materials used were poly(lactic acid) PLA and poly(lactic co-glycolic acid) PLGA, mixed in different proportions. For comparison, membranes where GS was directly dispersed were also made, as well as membranes where half the GS was freely dispersed and half was encapsulated in MSN's.

The MSN's – before and after the GS loading - were physically characterized by way of nitrogen adsorption/desorption measurements, which allowed for the determination of the specific area, pore volume and average pore size. Additionally, the quantification of the immobilized GS in the nanoparticles was determined by way of thermogravimetric analysis, having obtained a loading of 30% (w/w). The nanofibrous membranes were characterized by Scanning Electron Microscopy (SEM), water contact angle determination, *in vitro* release and microbiological tests.

The *in vitro* release tests showed that the membranes that possessed GS loaded MSN's presented a more controlled and prolonged release of the drug, in comparison with the ones with free GS dispersion. The polymer composition was also shown to affect the release kinetics, especially on the membranes with MSN's. Additionally the microbiological tests proved that the GS kept its antibiotic capabilities even after being subjected to several processes like encapsulation into MSN's and later electrospinning.

Resumo

Este trabalho tem como objectivo o desenvolvimento de membranas nanofibrosas de base polimérica capazes de actuar como um sistema de libertação controlada e localizada do antibiótico sulfato de gentamicina (GS). Pretende-se que estes sistemas possam ser implantados aquando de uma cirurgia ortopédica, de forma a prevenir ou tratar o desenvolvimento de uma eventual infecção óssea no período pós-cirurgico.

A libertação controlada e localizada de fármacos tem como objectivo desenvolver sistemas de entrega de fármacos que possuam a capacidade de controlar, temporal e espacialmente, a concentração de fármaco disponível no organismo. A maioria dos sistemas de libertação controlada (SLC) desenvolvidos é de base polimérica, isto é devido à variedade de propriedades químicas, físicas e biológicas exibidas por este tipo de materiais e à facilidade do seu processamento. Um método de processamento de polímeros considerado bastante atraente para a preparação de SLC é a electrofiação, uma técnica que permite produzir fibras de base polimérica com diâmetros desde alguns micrómetros até algumas centenas de nanómetros. Estas estruturas apresentam uma elevada relação de área superficial por volume, o que é favorável à incorporação e libertação de fármacos. Por outro lado esta característica também favorece uma libertação inicial muito rápida e extensa do fármaco incorporado, o que pode não ser desejável para alguns tipos de terapia. Este problema é mais acentuado quando o fármaco que se pretende encapsular é hidrofílico, como é o caso do antibiótico sulfato de gentamicina. Uma possível solução para este problema vem na forma de nanopartículas de sílica mesoporosa (MSN's), um material muito investigado para a imobilização e libertação de fármacos.

Assim, e numa tentativa de obter membranas nanofibrosas com uma libertação de GS de forma mais controlada e por intervalo de tempo relativamente longo, neste trabalho imobilizou-se GS em nanopartículas de silíca mesoporosa. Estas partículas foram então dispersas numa solução polimérica que posteriormente foi sujeita a electrofiação, obtendo-se dessa forma a incorporação das MSN's carregadas com a GS nas nanofibras produzidas. Como material poliméricos utilizou-se os polímeros poli(ácido láctico) PLA e poli(ácido láctico-co-glicólico) PLGA, misturados em diferentes proporções. Para comparação, preparam-se também membranas onde o antibiótico foi directamente disperso na solução polimérica, e membranas em que metade da GS incorporada se encontrava imobilizada nas MSN e a outra metade na forma livre.

As MSN's- antes e depois do carregamento com GS- foram caracterizadas do ponto de vista físico através de medidas de adsorção/desorção de azoto, o que permitiu a determinação da área específica, volume de poro e tamanho médio de poro das partículas. Adicionalmente, a quantificação da GS imobilizada nas nanopartículas foi determinada por meio de análises termogravimétricas, tendo-se obtido uma percentagem de carregamento de 30% (p/p). As membranas nanofibrosas produzidas foram caracterizadas por SEM, determinação de ângulos de contacto com a água, testes de libertação *in vitro* e testes microbiológicos.

Os resultados dos testes de libertação *in vitro* demonstraram que as membranas nanofibrosas com a GS imobilizada nas MSN apresentavam uma libertação mais controlada e prolongada do antibiótico, em comparação com as membranas onde a GS se encontrava na forma livre. Também se verificou que a composição polimérica da membrana afecta a cinética de libertação do antibiótico, especialmente nas membranas com MSN. Adicionalmente os testes microbiológicos provaram que a GS manteve a sua capacidade antibacteriana mesmo após ter sido sujeita a vários processos como a encapsulação em MSN's e posteriormente a electrospinning.

Contents

Symbols and Abbreviations

BJH – Barrett-Joyner-Halenda

DMF – Dimethylformamide

GS – Gentamicin Sulfate

MSN – Mesoporous Silica Nanoparticle

np-Si – Silica nanoparticle

npSi-GS – Gentamicin loaded Silica nanoparticle

OPA – ortho-Phthalaldehyde

PBS – Phosphate buffer saline

PCLA – poly (L-lactide-co-caprolacone)

PEG – poly (ethylene glycol)

PLA – poly (lactic acid)

PLGA – poly (lactic co-glycolic acid)

PMMA – poly (methyl metacrilate)

SEM – Scanning Electron Microscopy

TGA – Thermogravimetric Analysis

UV – Ultra Violet

VIS – Visible

List of Figures

List of Tables

Chapter 1

Introduction

1.1 Motivation

Drug administration is a key part of medical treatment, and therefore the need for constant development of drugs and their delivery is ever present. Applications dealing with antibiotic delivery in post-surgery scenarios, where prevention of infection onset is of the highest priority, present one of the most important therapeutic areas as they deal with weakened tissues where infection can easily take a foothold [1]. Thus it is no surprise that development of drug delivery in these applications is noticed.

Out of the developments in this area, controlled localized drug delivery is one of the most prominent. These systems are, as the name implies, able to deliver the drug at a controlled rate that can be defined according to the biological needs at a given situation. This not only reduces the toxicity dangers of drug administration but improves the therapeutic effectiveness as well due to a tighter dose control [2].

Controlled drug delivery requires the use of a vehicle, that is to say a base platform on which the drug is incorporated and from where it is later released. For this role the most common materials used are without doubt polymers. When speaking of polymeric based drug delivery systems and their application, one important aspect to take into consideration is the method through which they are produced, as it will, in great part, determine the structure and key characteristics of the drug delivery system.

One method with great potential for producing polymeric structures for drug delivery applications is electrospinning. This stems from the nanofibrous structure this method is able to produce and the high surface area this kind of structure presents. This high surface area is attractive when talking about drug delivery applications. Adding to this, electrospinning is a simple and versatile method, where a wide variety of polymers can be used and where the drugs can be easily incorporated in the polymeric nanofibers. Furthermore it is a cost effective method, and able to be scaled up to industrial levels, thus attracting more attention from the financial point of view as well [3].

With all this in mind, the motivation behind this work is to develop, or at least provide the beginning for the development, of a membrane with controlled and

localized antibiotic delivery capabilities. The intended final use for this membrane is as a means to deliver antibiotics on post-ostheosurgery sites, as an easy and effective countermeasure for infection of the vulnerable bone tissue. By using GS, an effective antibiotic against *Staphylococcus aureus* one of the most common bacteria behind ostheomyelitis [4], in conjunction with electrospinning, this work aims to result in a platform that is effective in the prevention of infection as well as being realistically feasible on a large scale.

1.2 Objectives

The main objectives of this work are:

- Production of electrospun nanofibrous membranes, based on the biocompatible and biodegradable polymers poly(lactic acid) PLA and poly(lactide co-glycolide) PLGA, for controlled and localized release of Gentamicin Sulfate (GS);
- Encapsulate GS into mesoporous silica nanofibers, and add them to polymer solutions to be electrospun;
- Determine the structural characteristics of the membranes;
- Obtain the release profiles for all the membranes;
- Observe the differences between the release profiles;
- Verify if the membranes have antibacterial activity.

1.3 Structure of this work

This work is comprised of five chapters and is organized as follows.

Chapter 1 presents a short introduction and motivation for the work, as well as the main objectives. A brief summary of the contents is also made.

Chapter 2 focuses on the theoretical background of the work. The fundamentals of controlled drug released as well as electrospinning are presented. This theoretical part is meant to familiarize the reader with the two main components of this work, as well as show how they come together.

Chapter 3 comprises the materials and methodology used in the experimental part of the work. The techniques used for production of membranes, as well as for analysis of their composition are laid out and explained. The methods used for characterization of the membranes, from their structure to their drug release effectiveness, are also presented.

Chapter 4 is dedicated to the results obtained from the analysis of the membranes, and their characteristics, as well as the discussion of those results. By the end of this chapter, all the experimental routes will hopefully be understood and supported by hard data.

Chapter 5 marks the end of the work. Here the conclusions taken from the results and suggestions for future work are presented.

Chapter 2

Theoretical Background

2.1 Controlled drug release

Localized controlled release of a drug is, as the name implies, the action of controlling the release of a drug, both spatially as well as in time. This can be achieved by administration of the drug in an appropriate controlled delivery system. The need for these systems comes from the fact that through traditional administration of drugs only a small fraction of the initial dosage arrives at its intended sites of action and/or receptors. In fact, the majority of the administered drug is destroyed while making its way towards the target site, by being taken up by other tissues or even by being metabolized too quickly in the target tissue, all this results in large quantities of wasted drug that end up serving no purpose [5].

Another side of the limitations of traditional administration is related to the concentration of the drug in the medium. The lack of specificity of the drugs themselves usually results in the need for a higher dose, and therefore an increase in the likelihood of the occurrence of unwanted side effects. Moreover, the hydrophobic properties of some drugs can make the ideal route for their administration unviable, which in turn makes achieving their ideal concentration on the target site very difficult. The development of controlled drug delivery systems seeks to eliminate, or at least minimize all of these issues [6].

Developing a system like this means that a number of factors must be taken into consideration:

- The physical, chemical, pharmacokinetic and pharmacodynamic properties of the drug;
- The physiological and biochemical barriers that come with the way for administration;
- The properties of the material to be used, especially its biocompatibility and, of course, the way it reacts to and with the drug;
- Lastly, the methods used in the manufacture of the system itself, as they also affect the behavior of the system.

2.1.1 Polymer based release systems

Due to their properties, variety, as well as versatility, polymers present the premium choice for the fabrication of a drug delivery system. However, for a long time, polymers were mainly used as additives to aid in the solubilization and stabilization of drugs, as well as mechanical support for the sustained drug release.

With the development of newer more advanced methods, the increased availability of different monomers previously unavailable, as well as expertise from other areas including biochemistry and nanotechnology, all contributed to advancements on the polymer area, creating new polymers that possess properties better suited for drug delivery applications, overall making them more effective at this role [7].

Nowadays polymers can be found with such specific properties, that the selection of the appropriate one for a specific purpose has become an increasingly more important and delicate step. However, any polymer to be considered for drug delivery applications must have certain basic fundamental characteristics without which their use is impossible for these applications. These are of course all the properties regarding biological interaction, of which the one that takes most prominence is biocompatibility with the tissues with which they will have contact. Also and if the polymer is biodegradable, the toxicity of the byproducts of its degradation must also be low. Due to the high water content of living tissue, the hydrophilic (or hydrophobic) characteristics of a polymer also present an important factor to be taken into consideration.

Another important factor that must be taken into account is the polymer's biodegradability. A biodegradable polymer is one that suffers chemical degradation from being in contact with living tissue, either through hydrolysis or enzymatic action, without producing any toxic (or otherwise harmful) biocompatible products, passible to be excreted through the natural processes of the body. Some polymers are not biodegradable, but bioerodible instead. What makes them different from the biodegradable type is that they do not suffer a chemical degradation, they are instead dissolved in the physiological medium and can either be excreted or remain in the organism.

2.1.2 Silica nanoparticles on drug release

Mesoporous silica nanoparticles are, as the name implies, a type of silica nanoparticles with a mesoporous structure, which is to say they possess pores with a diameter in the 2 to 50nm range. The beginnings of these nanoparticles date back to the early 1990's, from the discovery of the M41S family of mesoporous materials, and since then new mesoporous solids have been developed. Among them are the MSN's which are also part of the same family, and have presented a promising platform for drug delivery since then, mainly due to their ordered mesoporous structure, that presents good biocompatibility, surface functionality and chemical stability, allowing at the same time for the controlled release of a variety of different drugs [6].

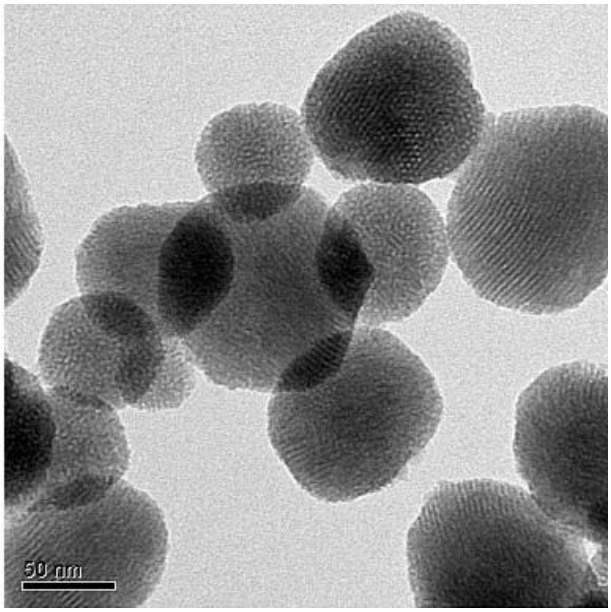

Figure 1 –Electron microscope image of mesoporous silica. [8]

In fact silica is present on various living organisms, from single celled ones to plants, which helps explain why it presents a high level of biocompatibility, especially when compared to metal oxides such as titania and iron oxide, which are also used for biomedical purposes. MSN's are also easily absorbed through endocytosis by living cells. Specifically this is due to the presence of silanol groups on the exterior of its mesoporous structure, as silanol may have affinity to phospholipids and these are actively absorbed by cells. These silanol groups are also responsible for the creation of a layer of apatite, similar to natural bone, when in contact with biological fluids, this characteristic allows them to be implanted on damaged bone. Also of note is the active

surface that MSN's possess, which allows for the creation of several surface properties for them which can be tailored more specifically to some drugs [6, 9].

Several studies have shown that smaller sized particles are better suited for drug delivery applications, where particles with a size in between 50nm and 300nm can be absorbed by living cells without danger of citotoxicity [10, 11]. Other studies also showed that particles on the 200nm or smaller size offer the best efficiency, and induce endocytosis, while particles on the microscale are more prone to phagocytosis but may not even be absorbed at all [12-14].

With this in mind it is clear that the mesoporous structure of MSN's is an attractive choice for drug encapsulation, as its size can be tuned in the 20nm to 500nm range in a controlled fashion. Adding to this, the pore size of the MSN's can also be finely tuned in the 2 nm to 6 nm diameter range with a very narrow size distribution. Also, these nanoparticles have a very large surface area and pore volume- usually around $1cm^3/g$- which allows for high drug loading capacities [10].

Another characteristic of MSN's that plays a role on its drug delivery behavior stems from its ceramic nature. Ceramics are notably slower to degrade than other materials used for drug delivery, namely polymers, and in fact they may not degrade at all. In MSN's this stems from the strong Si-O bond, which gives it more stability, namely added resistance to mechanical stresses and therefore MSN's are not prone to swelling like polymers. It also gives them a higher resistance to pH and temperature variations as well as degradation, which removes the need for other mechanical stabilization such as covalent linkers. This means that the drug release may be prolonged, as smaller quantities of drugs are released as an initial burst. This property is decisive for drug delivery processes that are dependent on diffusion, seeing as these are controlled through concentration differences of the mediums, and the concentration gradients can be kept for longer which of course means that the release window is also larger. Due to all of the properties shown, especially the tunable ones, MSN's can be and are applied to the delivery of various drugs. These include antibiotics, anti-inflamatories, and even chemotherapeutics [6, 13, 14].

Due to the nature of this work, the role of MSN's in the delivery of antibiotics will be given some detail. In the administration of antibiotics it is important to have a controlled and targeted release on the relevant tissue. This stems from the need to avoid possible resistance to the effects as well as have noticeable and adequate therapeutic effect. This requires a delicate balance in the quantity of the drug to be delivered into

the tissue, because of the adverse effects that can become apparent on the event of a dose which is too high, or of course the ineffectiveness of the antibiotic in the event of a dose too small.

2.2 Fundamentals of electrospinning

In this section the fundamentals of electrospinning are presented, the origins will be briefly explained, as well as the technique itself, and of course its applications especially in the field of controlled drug delivery.

2.2.1 Introduction

Electrospinning is a process for the formation of fibers on the micro and nanoscale using electrical forces.

The roots of electrospinning go back as far as the 17th century, specifically to William Gilbert with his work "On the Magnet and Magnetic Bodies and on that Great Magnet the Earth" where his observations on the effects of an electric charge on a fluid relate the formation of a structure that can be described as a *Taylor cone*, before the term was coined, and the ejection of fluid droplets from it. The term *electrospraying* was given to the phenomenon and was, in the late 19th century, further developed by C.V. Boys who named it *electrical spraying* [15]. Boys used an apparatus described as "a small dish, insulated and connected with an electrical machine", and observed that as the liquid reached the edge of the dish, fibers could be drawn from a few different melts [16].

Even with all these discoveries, it wasn't until 1934, by the hand of Anton Formhals, that successful electrospinning was achieved, Formhals reportedly electrospun a cellulose acetate thread from an acetone solution. Studies on the method were continued over the subsequent years, until 1964 when Sir Geoffrey Taylor studied and published a number of works on the process and developed a mathematical model for it, as well as observing and describing his observations on a conical structure that was formed when a liquid was subjected to an electrical charge. This structure we know nowadays as the *Taylor cone*, so named in his honor. Following Taylor's works, a number of studies were made on electrospinning, of which one made by the Reneker group at the University of Akron deserves special notice, as it demonstrated the

formation of fibers from a number of organic polymers and popularized the term electrospinning [15].

Since then there has been an increasing number of publications on electrospinning, especially since the year 2000, owing to the simplicity, versatility as well as potential uses of the technique [17].

2.2.2 Technique

When a high voltage of sufficient intensity is applied to a liquid droplet, it becomes charged and the electrostatic repulsion is able to counteract the surface tension. It is on this event that electrospinning is based [18].

Increasing the intensity of the electric field results in the stretching of the surface of the drop, which takes a conical shape that, as has been said in the previous section, is named the *Taylor cone*. When the strength of the electrical field surpasses the surface tension, a continuous jet of liquid is ejected from the *Taylor cone* [19, 20].

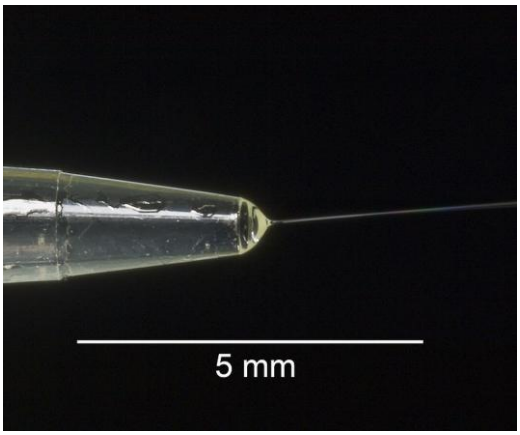

Figure 2 – Detail of the Taylor cone. [21]

Upon leaving the *Taylor cone*, the jet of liquid travels through the air and goes through what is called whipping instability, stretching and accelerating towards the direction of a grounded collector, as well as drying in flight. This instability is a result of small bends that are present on the initial phase of the jet. Because of these bends the surface charges on the perimeter of the jet create a dipolar momentum, resulting in a torque that bends the jet and continues doing so the further downstream it goes, the jet's diameter is again decreased as the solvents evaporate [22, 23]. When the liquid is a polymeric solution with an appropriated viscosity, during the jet trajectory between the

Taylor cone and the collector continuous ultrafine polymeric fibers are formed and deposited in the ground collector. These fibers have typical diameters that range from a few micrometers to a few hundred nanometers. These fibers, called electropsun fibers, have amazing properties deriving from their small diameter as well as high surface to mass ratio [18, 24].

The basic setup of electrospinning is very simple. It is composed of a high-voltage DC power supply connected to a spinneret (usually a hypodermic needle), a counter electrode which serves as the collector for the fibers, and a mechanism (usually a syringe pump) that feeds the spinneret with a stream of the polymeric solution [23].

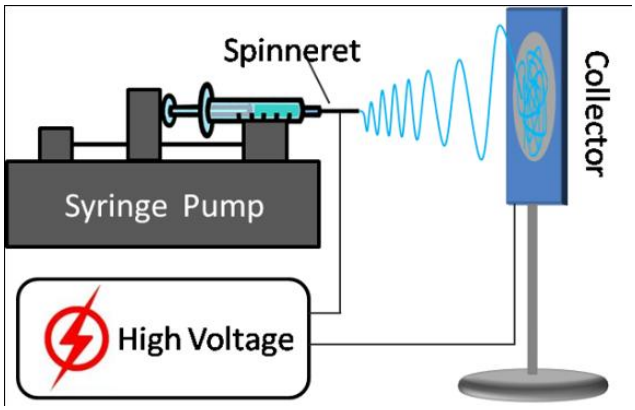

Figure 3 – Typical electrospinning setup. [25]

Due to the way the whole process works, there are a number factors that influence the final geometry and morphology of the formed fibers. These aspects are related to different parts of the process as a whole, including the properties of the polymeric solution itself, such as the viscosity, the polymer molecular weight, conductivity, dielectric constant and surface tension. Other factors include the flow rate, distance from the needle to the collector, and the design of the needle as well as the collector itself. Aside from these, ambient aspects such as temperature and particularly humidity also affect the process, and must be monitored and controlled as best as possible [23, 26].

2.2.3 Applications of electrospinning in drug delivery

The unique properties exhibited by the electrospun fibers, allied with the versatility and simplicity of the electrospinning technique itself, makes electrospun materials attractive for various applications, from textile manufacture, filtration and, of course, medical applications, where the electrospun fibers are used as scaffolds in the engineering of several tissues, like skin, cartilage, blood vessels and even nerves. Electrospinning also finds use in the area of drug delivery, which will be given special attention due to the nature of this work.

The high surface area to volume ratio present in the fibers manufactured with electrospinning makes it a good candidate for drug delivery applications. The already mentioned simplicity of the technique as well as the diversity of choice in the materials, where biodegradable as well as non biodegradable materials are viable, only make it more convenient and therefore attractive for this application. The first report of electrospun fibers used as a drug delivery platform dates back to 2002, by the hand of Kenawy et al [2], and since then researchers have paid attention to electrospinning as a drug delivery platform [26].

A wide variety of polymers, and co-polymers have been used for drug delivery applications [3]. Among them the most popular ones for this type of application are PLA [2, 27, 28], PLGA [29, 30], poly(L-lactide-co-caprolacone) PCLA [23], poly(methyl metacrylate) PMMA[1, 4, 29, 31-33], and poly(ethylene glycol) PEG [27], which have been featured in a number of studies. In this work PLA and PLGA were combined into mixtures with different configurations, explained in the methods sections.

A few different methods can be used for the incorporation of drugs in the electrospun fibers. They include coating, coelectrospinning of the drugs and the fibers (also named embedding), and encapsulation by coaxial and emulsion electrospinning. The release kinetics of a drug from an electrospun delivery system can be controlled by selecting the most adequate polymer(s) and solvents to use, selecting a specific loading method, as well as by manipulating the operational variables of electrospinning [26, 34].

The coating method, as the name implies, consists on adsorbing or chemically attaching the drug molecules directly onto the surface of the formed fibers. In the co-electropinning, method the drugs are dissolved in the polymer solution and are then

electrospun along with the polymer itself. When it isn't possible to find a solvent or mixture of solvents that can dissolve both the polymer and the drug, the drug particles can be simply dispersed in the polymer solution.

The co-electrospinning method presents the advantage of being able to create drug loaded polymeric fibers in one single step, and thus being simpler than the coating method, as well as resulting in having the drug embedded in the fibers [35]. The release of the drug occurs via diffusion, or sometimes by diffusion coupled with the degradation of the material when working with biodegradable materials. This means of course that the degradation of the polymer plays a role on the release rate, and therefore by selecting the chemical composition of the polymers the release rate can be controlled.

The encapsulation form of drug loading is usually used for the incorporation of macromolecules into electrospun fibers. Two methods have been successfully developed:

The coaxial electrospinning, that involves the use of two (or more) coaxial nozzles, and the emulsion electrospinning, which involves the electrospinning of polymeric emulsions using a single nozzle. Both methods produce core-shell structured electrospun fibers where the drug is encapsulated in the core and isolated from the release environment by a polymeric shell. This means that, theoretically, these methods can reduce the initial burst release of the drugs [26].

In this work the co-electrospinning and encapsulation methods were both used, the latter involved the use of mesoporous silica nanoparticles, in conjunction with GS, an antibiotic.

The choice of MSN's to combine with the electrospun polymers was not a hard one to make. Aside from their merits regarding drug delivery, which were explored in the controlled release section, MSN's have been successfully incorporated into electrospun polymer nanofibers over the years. Moreover the characteristics and the drug release behavior of MSN's show that they present a good choice for the release of antibiotics [28, 30, 36].

As mentioned before, the localized release of antibiotics removes the problem of over dosage to some extent, seeing as all of the drug dose will be released *in situ* as opposed to dispersed in the whole body and subjected to being absorbed in the wrong tissues. It also solves the opposite problem, that of under dosage, because with the

release being localized the whole dose will be released into the relevant site. Besides these dose related issues, another important aspect of antibiotic administration is related to the need for a continued administration, since for antibiotic drugs to be effective the dosage must be kept fairly constant throughout a specific period of time. As has been shown before MSN's can lengthen the release window of drugs, reducing the occurrence of an initial release burst and spreading out the release in time. In essence they can slow the release of the drug and make it so it releases at a more even rate through a set period of time, therefore being a good choice for use in the release of antibiotics.

Chapter 3

Methods

MSN's have been proven, as it was stated before, to slow the release rate of drugs on controlled release systems, and therefore to lengthen the release window, which was one of the main goals of this work.

As such, silica nanoparticles were used to encapsulate the GS and afterwards electrospun simultaneously with the polymers as they were a part of the solution. The Poly(L,D-lactic acid) (PLA) Ingeo^{TM}2002D, with a reported average Mw of approximately 130,000 g/mol [37] was purchased from NatureWorks (USA). The poly(D,L-lactide-co-glycolide) (PLGA, L/G 50:50, ester terminated, Mw 54,000 - 69,000) and the mesoporous silica nanoparticles, with an average particle size of 200 nm and average pore size of 4 nm were bought from Sigma-Adrich. Gentamicin sulfate salt (potency ≥ 590 μg gentamicin base per mg) was purchased from Alfa Aeaser. Other reagents, namely, o-phthalaldehyde, chloroform, N,N-dimethylformamide (DMF), isopropanol, and 2-mercaptoethanol were all of analytical grade and were obtained from several suppliers.

3.1 Loading of GS into MSN's

In order to have GS loaded into the MSN's, 500 mg of MSN's were dispersed in 5ml of GS aqueous solution (50mg/ml) and left under magnetic agitation overnight. Afterwards, the suspension was centrifuged, the aqueous phase was discarded, and the isolated drug loaded MSN's were freeze-dried.

3.2 Preparation of polymer mixtures

Both PLA and PLGA were used in all formulations, although in different proportions. The PLA/PLGA proportions used, in weight, were of 3:1, 1:1 and 1:3, designated here as 75PLA/25PLGA, 50PLA/50PLGA, 25PLA/75PLGA. In all mixtures, the total polymer weight was of 1g. The polymers were dissolved in a mixture of chloroform and DMF, where the quantity of DMF was always a third of the quantity of chloroform.

The GS was incorporated in the mixtures by the dispersion of a certain quantity of GS loaded MSN's in the polymeric solutions (mixtures 75PLA/25PLGA-Si, 50PLA/50PLGA-Si and 25PLA/75PLA-Si) or, alternatively, by the direct dispersion of the drug into the polymeric solutions (75PLA/25PLGA, 50PLA/50PLGA, 25PLA/75PLA). In the last two formulations (50PLA/50PLGA-Si-5% and 50PLA/50PLGA-Si-15%) half of the added GS was dispersed in the form of "free" GS and the other half loaded in the MSN's.

The composition of all the mixtures used to fabricate the electrospun materials are resumed in Table 1.

Table 1 – Composition of the mixtures subjected to electrospinning.

Mixture	Polymer Weight (g)	Solvent volume* (ml)	GS (mg)	GS loaded MSN's (mg)	% GS#
75PLA/25PLGA	0,75 PLA+ 0,25 PLGA	10	50	-	5
50PLA/50PLGA	0,5 PLA + 0,5 PLGA	8	50	-	5
25PLA/75PLGA	0,25 PLA+ 0,75 PLGA	7	50	-	5
75PLA/25PLGA-Si	0,75 PLA+ 0,25 PLGA	10	-	125	3,8
50PLA/50PLGA-Si	0,5 PLA + 0,5 PLGA	8	-	125	3,8
25PLA/75PLGA-Si	0,25 PLA + 0,75 PLGA	7	-	125	3,8
50PLA/50PLGA-Si-5%	0,5 PLA + 0,5 PLGA	8	25	84	5
50PLA/50PLGA-Si-15%	0,5 PLA + 0,5 PLGA	8	75	250	15

* Mixture of chloroform and DMF, 3:1 (v/v)

Relatively to the polymer weight (1 g) and considering a GS loading of 30% (w/w) in the GS loaded MSN's.

3.3 Fabrication of the drug loaded electrospun materials

The electrospinning setup used in this work was of a very simple design. It used a NE-1000 Multiphaser syringe pump, on which a 10ml syringe was mounted. The syringe was connected to a metallic needle through a small diameter tube. The needle was mounted on a simple wood support, and was connected to a high-voltage power supplier (SL 10W-300W, Spellman) by a crocodile. The collector consisted of a flat square surface, grounded through a wire connected underneath it, and covered in tin foil at the times when electrospinning was conducted, as observable on Figure 4.

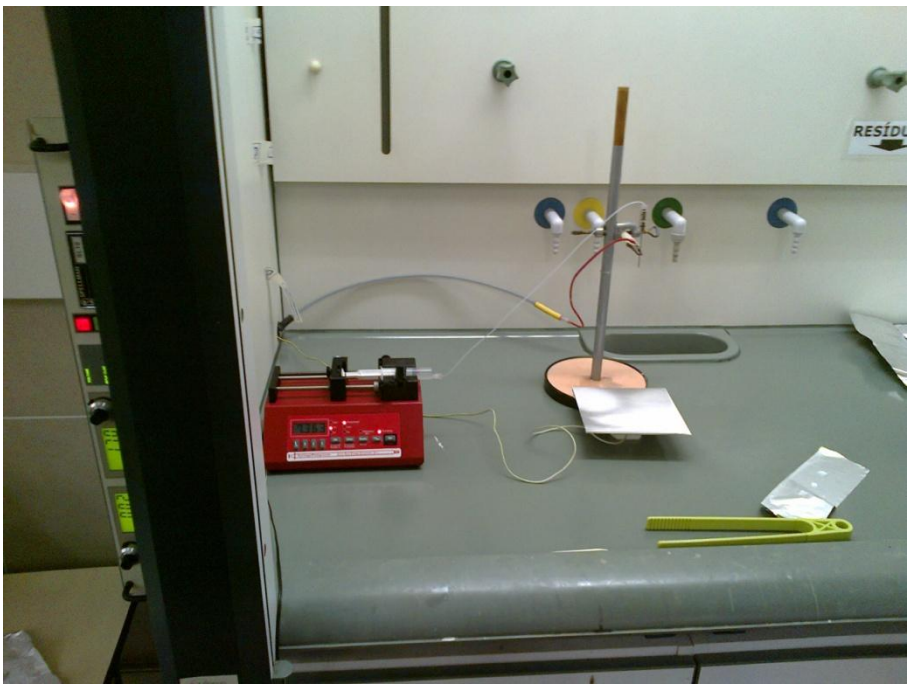

Figure 4 – Electrospinning setup used for this work, the power source can be seen on the left.

When conducting electrospinning the first step was to empty the needle and the tube that connected it to the syringe of air, to accomplish this the high-voltage supply was turned off and the syringe pump was set to a very high rate (this rate varied but was always set into the tens of ml/h). Once polymer solution began to drip from the needle into the collector, on which a small scrap of tinfoil was set, the pump was stopped the tinfoil scrap removed and the electrospinning proper could now take place. Afterwards the power supply was turned on (meaning a much higher care was now required) and usually set to 15kV, while the syringe pump was typically set to a rate of 2ml/h.

Notable exceptions to these settings were the solutions that were electrospun on days of high air humidity, which required a higher voltage setting of 17kV-18kV, and a lower pumping rate, usually reduced to 1,5ml/h. The last batch of polymer solutions were electrospun with 14kV and 2,5ml/h settings, the latter aimed at speeding up the process.

3.4 *In vitro* release tests

To observe the release profiles of the developed membranes, *in vitro* release tests were performed. With this purpose, rectangular pieces were cut out of the membranes and put in a phosphate buffer saline (PBS, pH= 7,4) medium, in an incubator which was

set to 37ºC. At predetermined periods of time, the release medium was removed and replenished with an equal amount of fresh PBS.

Samples of the fluid medium were taken on intervals that were the same for all tests. Several samples were taken on the first day, then every 24h for a week and every 48h for the following two weeks. Once this time period was finished, and all the samples had been taken, the membrane pieces that were in the release medium were dissolved in chloroform. The resulting solution was mixed with 3ml of PBS solution, centrifuged and, once the centrifugation was complete, the supernatant (aqueous phase) was carefully taken and put into vials. This process was repeated twice more for all the samples. This last step was done with the objective of extracting the GS that was still left in the membranes after the release time.

3.5 Quantification of GS by a UV/VIS spectrophotometric method

The GS in the samples taken during the *in vitro* release tests was quantified by a spectrophotometric method using a UV/VIS JASCO 550 spectrophotometer. Since GS does not absorb light in the visible (VIS) or ultra-violet (UV) region, an indirect method was used, that involves the reaction of GS with the UV absorbing reagent ortho-phtalaldehyde (OPA) [38].

First, an OPA solution, here designated by OPA reagent, was prepared by mixing:

- 0,42g of ortho-phtalaldehyde;
- 10 ml of methanol;
- 90ml of an aqueous solution of sodium borate 0,04M;
- 0,5ml of mercaptoethanol.

The reagent must be left to stir for 24h in the dark, as it is sensitive to light and it is also only viable for three days, after which it no longer produces the intended reaction.

Once these 24h have passed, the samples could be prepared for the analysis in the spectrophotometer. The samples were prepared by mixing, directly in the plastic couvettes, the GS samples, the OPA reagent, and isopropyl alcohol, all of them in equal amounts (800 µL). The mixture was then allowed to react at room temperature for 30 minutes, and afterward the absorbance was registered at the wavelength of 332 nm. Standard gentamicin solutions with concentrations between 10 and 100 µg/mg, treated the same way, were used to construct a calibration curve.

As stated above, the use of a spectrophotometer produces absorption values on a given wavelength. The absorption values can be related to GS concentration in the solutions by the Beer-Lambert law.

The Beer Lambert law is a mathematical relation that correlates the attenuation of light through a material and the same material's characteristics. The law states that the absorbance and the concentration of a sample are linearly related to one another. It is written as:

$$A = \varepsilon l c$$

Where:

- ε is the absorption coefficient, units: $L.mol^{-1}.cm^{-1}$;
- l is the path length, units: cm;
- c is the concentration of the sample, units: $mol.L^{-1}$.

The standard spectrophotometer uses couvettes with a width of 1cm, and in fact it is also the case for the couvettes used in this work, and therefore this factor can be omitted. Seeing as ε is a constant specific to the material, and therefore known, from the value of absorbance or concentration the other value can easily be obtained.

As mentioned, in this work, five solutions were prepared parallel to the release samples taken before. These solutions were simply GS dissolved in a PBS medium, at different known concentrations, the absorbance values obtained for these solutions were used to construct a calibration curve. The correspondent linear regression provided the slope value that allowed the calculation of the concentration values of the samples that were tested.

Once the concentrations of the release samples were ascertained, it became easy to obtain the values for the quantities of GS released from the samples, as well as the quantities of the residue that was left still in the polymer membrane. These values then allowed for the construction of release profiles.

3.6 MSN characterization

To characterize the MSN's two methods were used, thermogravimetric analysis (TGA), and nitrogen adsorption/desorption. TGA allowed to ascertain the drug loading of the MSN's, while with the nitrogen adsorption/desorption analysis the surface

characteristics of the MSN's, namely the pore diameter distribution and pore volumes with and without GS loading were determined.

3.6.1 Thermogravimetric analysis

The weight loss in function of temperature for pure GS, pure silica MSN's, and GS loaded silica MSN's, was recorded from room temperature to 1200ºC and at a heating rate of 10ºC/minute, using a simultaneous thermoanalyzer SDT 600 (TA Instruments).

The obtained thermograms were then used to calculate the GS loading into the silica MNP's.

3.6.2 Nitrogen adsorption/desorption measurements

The surface area and pores size distribution of the nanoparticles was evaluated by nitrogen adsorption/desorption isothermal measurements performed on a Micromeritics ASAP 2000 analyzer. The surface areas were calculated based on the Brunauer-Emmett-Teller (BET) theory, while the pore volume and pore size distributions were obtained from the adsorption isotherm branch, using the Barrett-Joyner - Halenda (BJH) method.

3.7 Characterization of electrospun materials

Similarly to the MSN's, the electrospun materials also had to be characterized, this was done through (SEM) and water contact angle determination. SEM permitted the observation of the morphology of the materials, while the water contact angles allowed the determination of their hydrophobicity levels.

3.7.1 Scanning Electron Microscopy

All of the manufactured membranes were analyzed with SEM, in order to observe the morphology of the membranes as well as the way the MSN'S were distributed throughout the fibers. Additionally, some membranes were also analyzed after being immersed in PBS at 37ºC for a period of 15 days.

For this analysis, small squares were cut out of the membranes, placed on double-sided graphite tape, attached onto a metal support, and sputter-coated with gold.

Observations were performed with a JSM-5310 (JEOL, Japan) scanning electron microscope. SEM images were also used to make an assessment of the fibers diameters distribution by means of image analysis software (ImageJ).

3.7.2 Water contact angle determination

To evaluate the hydrophobicity/hydrophilicity character of the surface of the electrospun fiber materials, water contact angles measurements were performed. The measurements were made with a Dataphysics OCA-20 contact angle analyzer (DataPhysics Instruments, Filderstadt, Germany) using the sessile drop method. The materials were cut into strips attached to a glass slide, and placed in the sample stage. A droplet of deionized water (10 µl) was automatically dispersed onto the sample surface and its contact angle calculated by the software of the equipment. At least five independent measurements were performed for each type of material.

3.8 Release efficiency

As stated above, the use of a spectrophotometer produces absorption values on a given wavelength. Absorption values on their own do not hold much meaning, and therefore must be treated in order to obtain values that do, in this case values of the quantity of released GS as well as how much was left in the membrane. This treatment is made mathematically and uses the Beer-Lambert law.

3.9 Antimicrobial activity tests

Seeing the intended purpose of the membranes is to locally release an antibiotic in controlled quantities, it is necessary to verify that when incorporated in the fibers the GS keeps it's antibacterial effectiveness.

The antibacterial activity of the GS loaded fibers against *Staphylococcus aureus* was determined by a disc diffusion (Kirby Bauer method) assay according to the European Committee on Antimicrobial Susceptibility Testing (EUCAST; http://www.eucast.org). The *S. aureus* clinical isolated used was identified as susceptible to Gentamicin (results not shown). Briefly, *S. aureus* was grown overnight in Mueller-Hinton plates (Diagnostics Pasteur, France). A bacterial suspension (0.5 McFarland turbidity) was spread with a swab onto Mueller Hinton petri dishes. The

materials were cut in 7 mm-diameter discs and deposited in the centre of each plate. The plates were incubated at 35 ºC and, after 24h the inhibitory effect of each disc was observed and evaluated by measuring the diameter of the inhibition zones, as observable in figure 5.

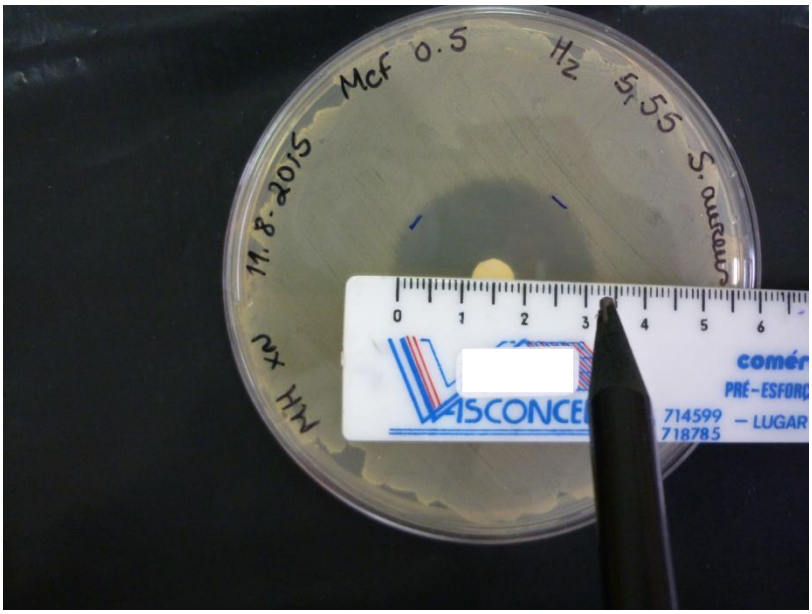

Figure 5 – Method used for the antimicrobial activity test.

Chapter 4

Results

In this section the results pertaining to the methods listed in the previous section are presented, as well as some observations on the immediate analysis of those results. The final conclusions to be taken from these results are presented on the section following the present one.

4.1 Nanoparticles physical characterization

The surface area and pore size of the MSN's will in great part determine the drug loading capacity of the nanoparticles and the drugs release kinetics. For this reason the surface area, the pore volume and the distribution of pores sizes of the MSN's were determined by nitrogen adsorption/desorption measurements, for the blank nanoparticles and the GS loaded nanoparticles. The results of this analysis are shown on figures 6 and 7, as well as on table 2.

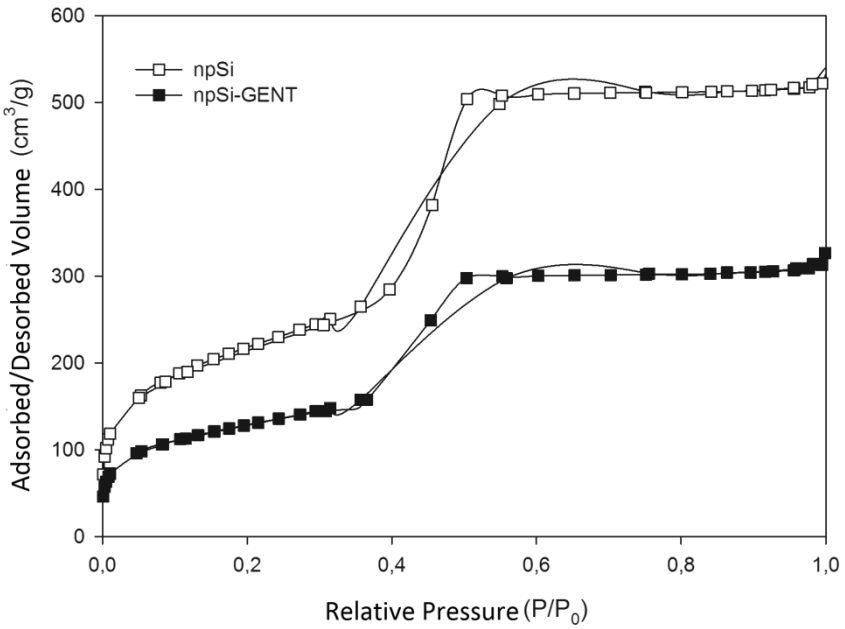

Figure 6 – Isothermal graph for nitrogen adsorption/desorption.

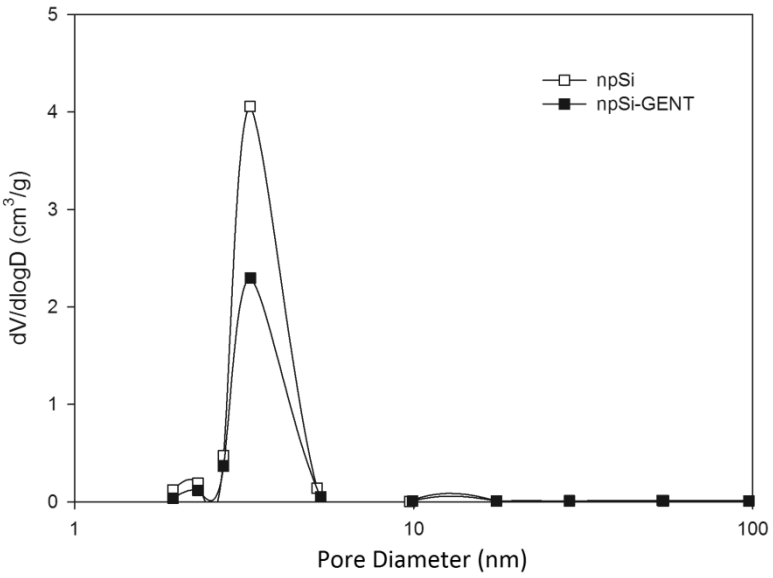

Figure 7 – Graph for the distribution of pore diameter for the MSN's.

Table 2 – Nitrogen adsorption/desorption data.

	S_{BET} (m^2/g)	*Vp* (cm3/g)	*Dp* (nm)
MSN's	763	0,860	3,3
GS loaded MSN's	449	0,515	3,4

The table shows that the MSN's have a high surface area with 763m^2/g and relatively large pore volume of 0.860cm^3/g. When loaded with GS particles both these values suffer a reduction, this is of course what is expected seeing as the once empty pores now contain GS particles that take up space. What is interesting to note is that after the GS addition both the volume and the surface area suffer a reduction of just over 40%, which shows that not even half of the pores' capacity is taken up by the GS, meaning that it could theoretically be possible to load the MSN's with a much higher quantity of GS. The pore diameter change in between the two MSN's, the GS loaded one and the free MSN's, is a very small difference and is in fact negligible.

4.2 Quantification of the GS loaded into the MSN's

In the production of the GS loaded fibers, the quantity of GS to be loaded into the membrane must be known, as the drug dose is one of the main factors in any drug administration.

Apart from this, in the perspective of the study the quantity of GS to be loaded into the fibers must be known to allow for the construction of the release profiles. When dealing with direct dispersion of the GS in the polymer solutions this is not an issue, as the quantity of GS is known from the start, however this is not the case for the GS loaded into the MSN's.

When loading the MSN's with GS the quantity added to the solution is known, however how much GS is actually encapsulated into the MSN's is not, and therefore this quantity must be determined. This was done through the use of a thermogravimetric analysis, which then allows for the mathematical determination of the quantity of GS encapsulated in the MSN's.

Figure 8 presents the weight loss profiles in function of temperature- from environment temperate to 1200ºC - of the pure gentamicin sulfate (GS), unloaded MSN's (npSi) and gentamicin loaded MSN's (npSi-GS).

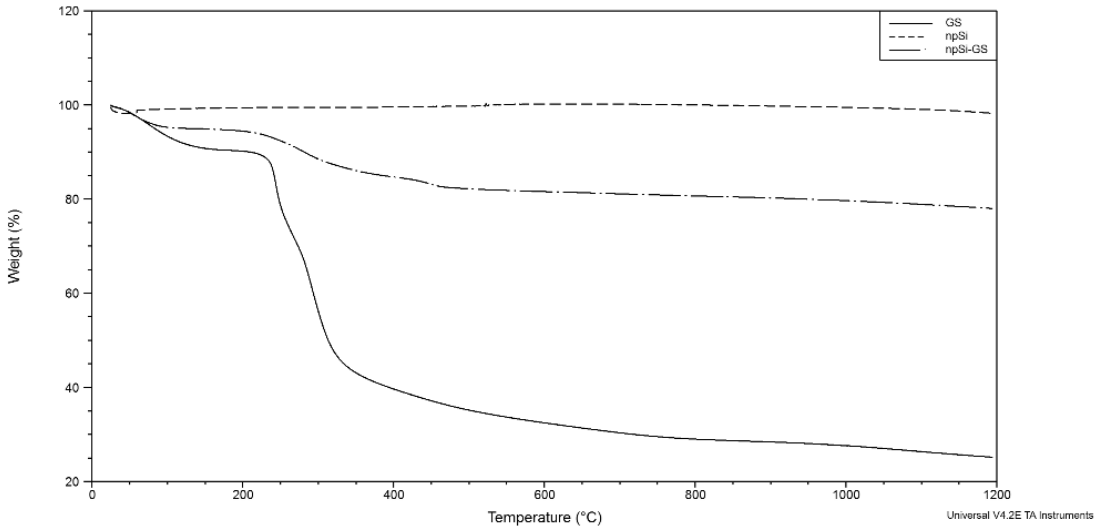

Figure 8 – TGA graph for GS, MSN's, and GS loaded MSN's.

The graph shows that the silica nanoparticles do not lose any mass during the course of the whole test, this is due to the inorganic nature of this material. Contrarily, the GS thermogram presents two main steps of weight loss: one around 100ºC,

attributed to the evaporation of water bound to the antibiotic molecules, and another situated between 250 and 350ºC, that can be ascribed to the thermal degradation of the drug. After this second step, the weight decreases slowly until only about 25% of the initial GS mass is left at 1200ºC. This remaining mass is probably due to inorganic salts associated with the drug that didn't suffer degradation. The main step of weight loss in the GS loaded nanoparticles (np-Si-GS) happens in the degradation zone of GS (250-350º), corresponding to the thermal degradation of the antibiotic immobilized in the particles.

Considering the final weights of the samples and through a mass balance the quantity of GS loaded into the nanoparticles was calculated (presented in Annex A). The obtained value was 30% (w/w).

4.3 Membrane structure

In the following section SEM images of the nanofibers are presented. They allow for the observation of the way the fibers are deposited and their orientation, as well as their morphology and, when applicable, the way the MSN's are placed throughout the fibers.

Figures 9 through 11 show pictures with different magnifications of the membranes loaded with free GS and composed of 25% PLA and 75% PLGA (Figure 9), 50%PLA and 50%PLGA (Figure 10) and 75%PLA and 25%PLGA (Figure 11). It is possible to observe the disposition of the fibers on the pictures on the left, and on the pictures of the right the surface morphology of the nanofibers. In the membranes with equal proportions of both polymers and with higher content of PLA a few round polymeric structures occur, designated as beads. They are more common on the fibers with more PLA. These structures are usually formed due to the polymer composition, more specifically to the higher concentration of certain polymers [26]. Such seems to be the case for PLA, seeing as the occurrence of beads in the images is concordant with the increase of PLA content.

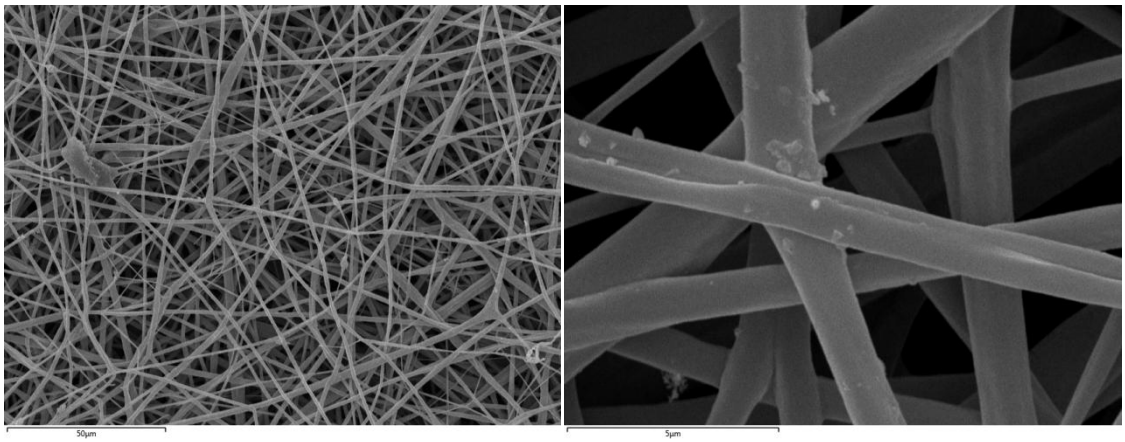

Figure 9 – SEM images for the membrane with 25%PLA content and without addition of MSN's. Magnification: 750x(left), 10000x(right).

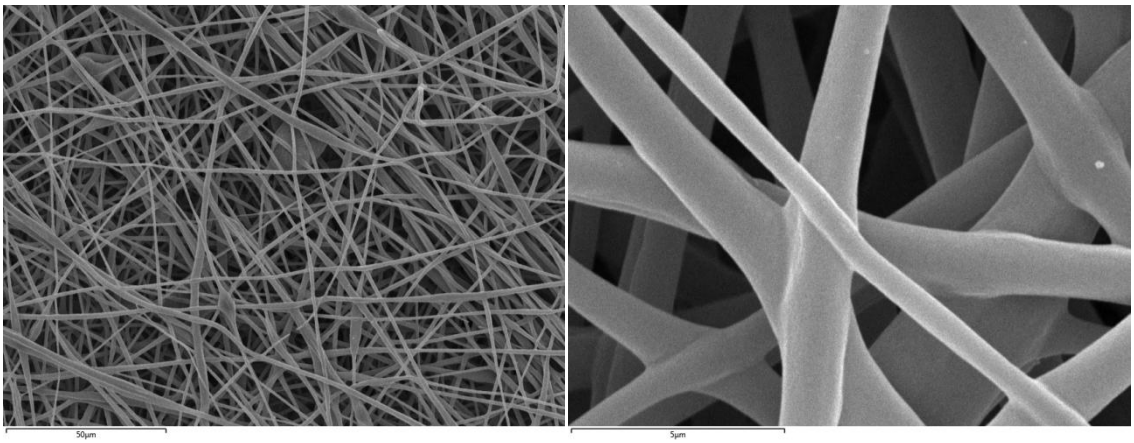

Figure 10 – SEM images for the membrane with 50%PLA content and without addition of MSN's. Magnification: 750x(left), 10000x(right).

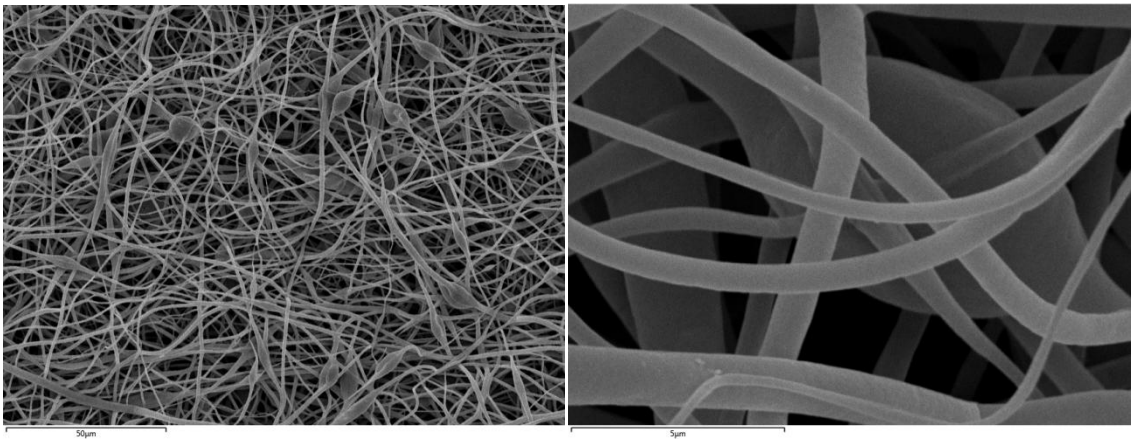

Figure 11 – SEM images for the membrane with 75%PLA content and without addition of MSN's. Magnification: 750x(left), 10000x(right).

The average diameters of the fibers, estimated by image analysis, are presented in table 3. From the table it is observable that the different polymer compositions result

in different fiber diameters. The values that were obtained show that the fibers with equal content of both polymers have a larger diameter than the others, while the fibers with the highest content of PLA have the smallest. With the addition of MSN's the diameters for all of the membranes increase but the highest diameter is now for the 25PLA/75PLGA membrane while the smallest remains for the 75PLA/25PLGA fibers. It is also apparent that the increase of the diameter is much less pronounced for the 75PLA/25PLGA which might be related to the way the MSN's is distributed on these fibers, this observation can be made on figure 14.

Table 3 – Average diameter of the fibers.

		Average fiber diameter (μm)	
		Without MSN addition	**With MSN addition**
Membrane Composition	25PLA/75PLGA	1,08 ±0,17	1,68 ±0,16
	50PLA/50PLGA	1,22 ±0,10	1,47 ±0,27
	75PLA/25PLGA	0.90 ±0,10	0,96 ±0,17

As can be seen in the images with higher magnifications, the surfaces of the nanofibers are smooth, with no visible pores. Also, on the surface of the fibers with the lowest amount of PLA (Figure 9) it is possible to observe some particles that are probably GS particles that were not incorporated inside the fibers. For the other compositions these particles were less visible or absent.

Figures 12 through 14 show the SEM images for the GS-silica loaded membranes. As it can clearly be seen the polymer agglomerates are still present for the fibers with the higher quantities of PLA. Also, on all of them it is possible to observe agglomerates of MSN particles, partially embedded on the fibers.

The images show that the polymer composition may also influence the disposition of the MSN's on the fibers, as the fibers with higher content of PLA (figure 14) show the formation of bigger agglomerates of silica nanoparticles. Thus, on the first set of images (figure 12) we can see that the MSN's are more loosely dispersed, while on the second case (figure 13) a few larger agglomerates can be seen, and on the last case (figure 14) there are less but larger agglomerates of MSN's. This might relate to the differences of release behavior that will be shown later on in this section.

While it might be difficult to conclude from observation of the images, the values on table 1 indicate that the diameter for these fibers is larger than it was for their MSN-less counterparts. This might be due to the presence of the MSN's inside the fibers, which would add volume and size to the fibers. While this is not completely obvious from observation of the images they do show that the MSN's adhere well to the polymer fibers and some are partially absorbed into them (observable in figure 13). Therefore it is not farfetched to assume that some MSN's are included inside the fibers themselves, and therefore adding to their size.

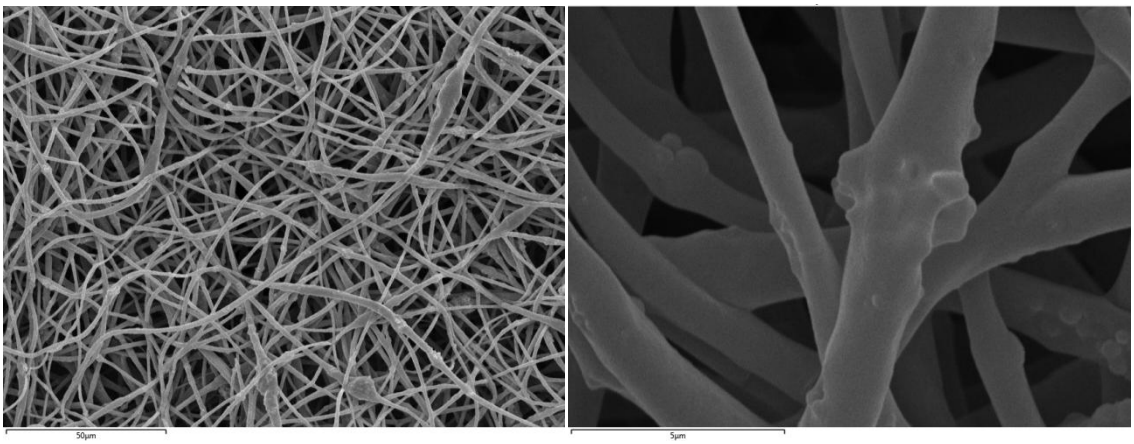

Figure 12 – SEM images for the membrane with 25%PLA content and addition of MSN's. Magnification: 750x(left), 10000x(right).

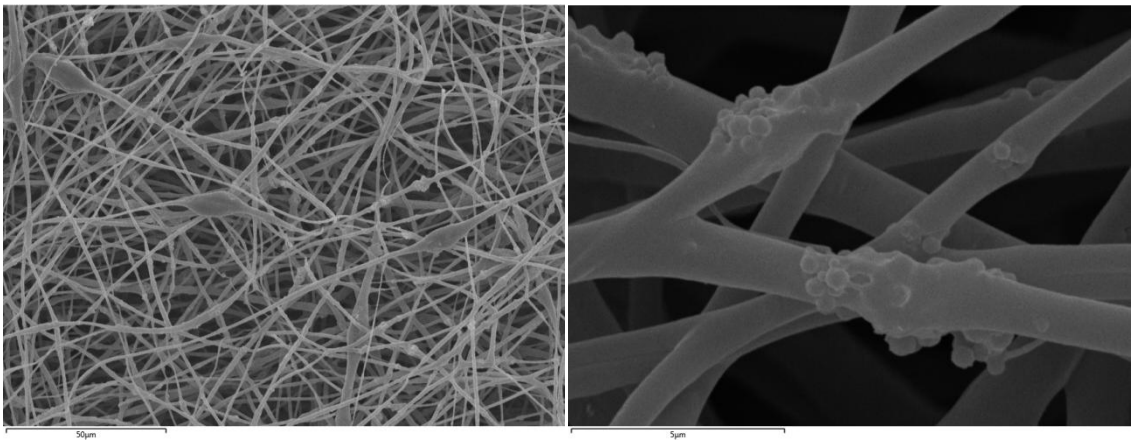

Figure 13 – SEM images for the membrane with 50%PLA content and addition of MSN's. Magnification: 750x(left), 10000x(right).

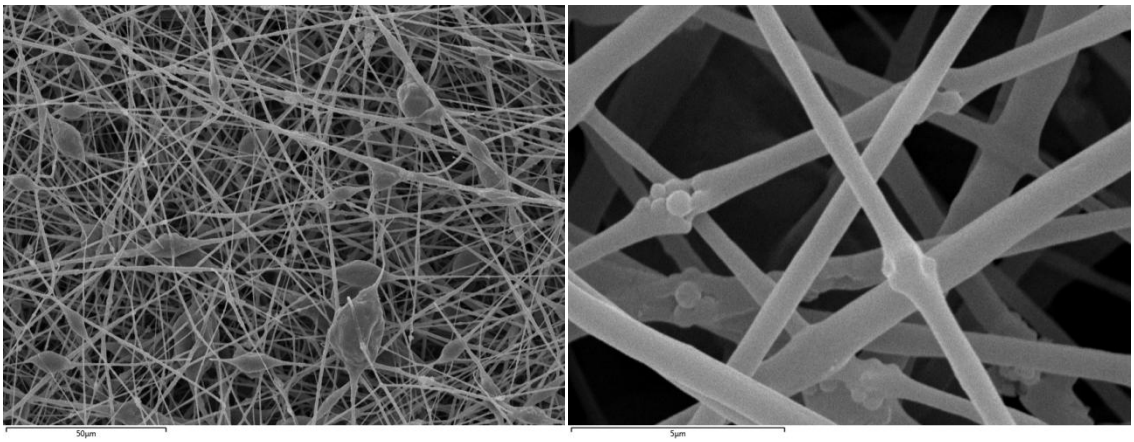

Figure 14 – SEM images for the membrane with 75%PLA content and addition of MSN's. Magnification: 750x(left), 10000x(right).

The images that follow (figures 15 and 16) are for the membranes with the hybrid loading of GS, with both dispersion of free GS and GS loaded MSN's, and fabricated with 50%PLA and 50%PLGA. It is necessary to note the omission of the SEM images for the fibers with 10% loading of GS. This is due to the fact that those membranes suffered contamination from a source still unknown at the time of the elaboration of this work. The contamination only made itself known when the samples were being prepared for analysis in the spectrophotometer, regardless, the results from their analysis could not be taken into consideration due to this occurrence.

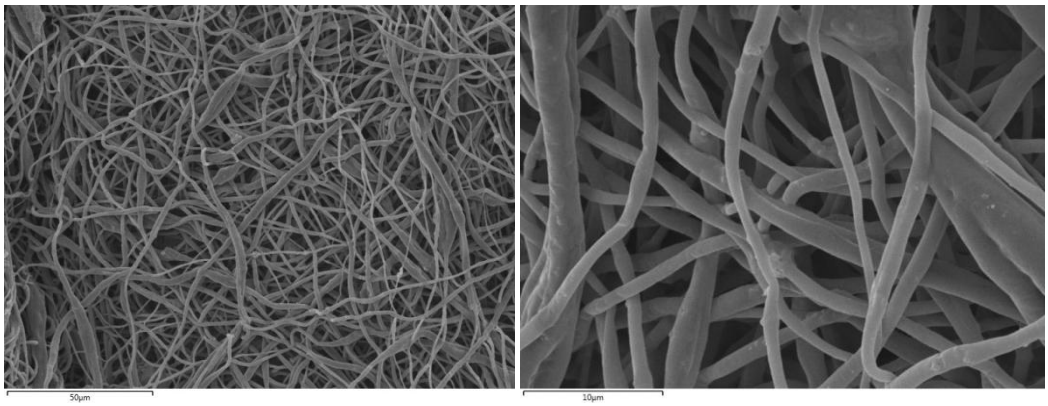

Figure 15 – SEM images for the membrane with a hybrid GS load method of 5%. Magnification: 750x(left), 3500x(right).

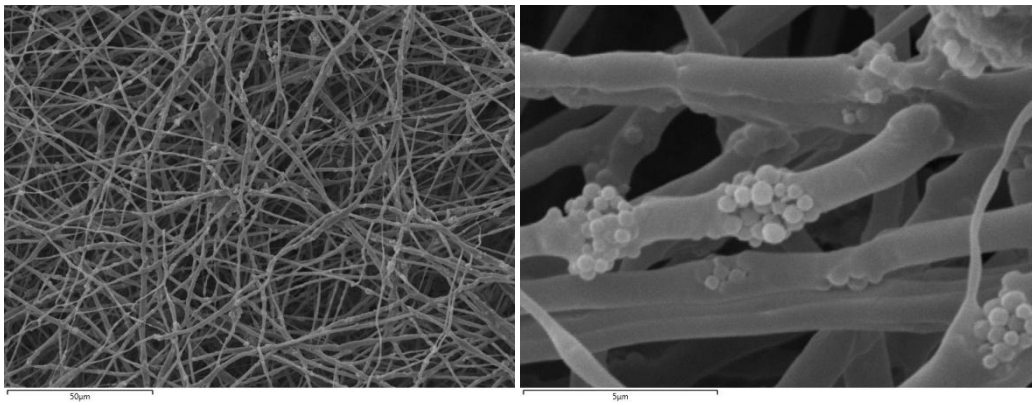

Figure 16 – SEM images for the membrane with a hybrid GS load method of 15%. Magnification: 750x(left), 10000x(right).

These membranes are very visually similar to the previous ones, which is of course to be expected as there is nothing new in their basic composition. The most notable visual difference between these membranes and the ones shown previously is the coexistence of what seems to be free GS particles and agglomerates of MSN's. It can easily be seen that, also as expected, in the membrane with 15% GS load there is a much larger quantity of agglomerates. In fact the images on the left for both of them illustrate this difference well, as on the 15% membrane MSN agglomerates have much more pronounced presence than on the 5% one. The free GS is more difficult to spot, however it can be seen on the second image for the 5% membrane, a few free GS particles are present along with a partially hidden agglomerate of MSN's.

The diameters for these fibers were also measured, the 5% load fibers averaged a 1,05±0,04μm while the 15% load fibers averaged 1,40±0,22μm. These values are relatively similar to the ones obtained for the 50/50 fibers with MSN's, which is to be expected considering their similar composition. Also to be expected is the smaller diameter of the 5% load fibers when compared to both the 15% load ones as well as the original 50/50 fibers with MSN's, seeing as the 5% load fibers contain a smaller quantity of MSN particles. However, the 15% load fibers show a similar diameter to the original 50/50 fibers with MSN addition, despite a much larger MSN content. Upon observation of the images for both (figures 13 and 16) it can be seen that the 15% load fibers show more agglomerates of MSN's. Therefore it seems that a maximum of MSN's located inside the fibers themselves is reached on both, and thus the excess MSN on the 15% load fibers forms the agglomerates.

As stated before a set of membranes were left in a PBS medium at 37ºC for two weeks, in order to verify the degradation of the membranes with time. The SEM images regarding these tests are shown in figures 17 through 19.

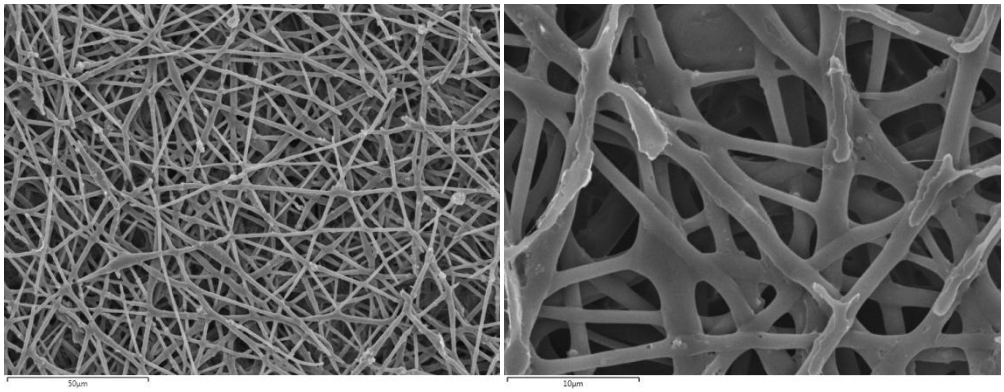

Figure 17 – SEM images for the membrane with 25%PLA content and addition of MSN's, after two weeks. Magnification: 750x(left), 3500x(right).

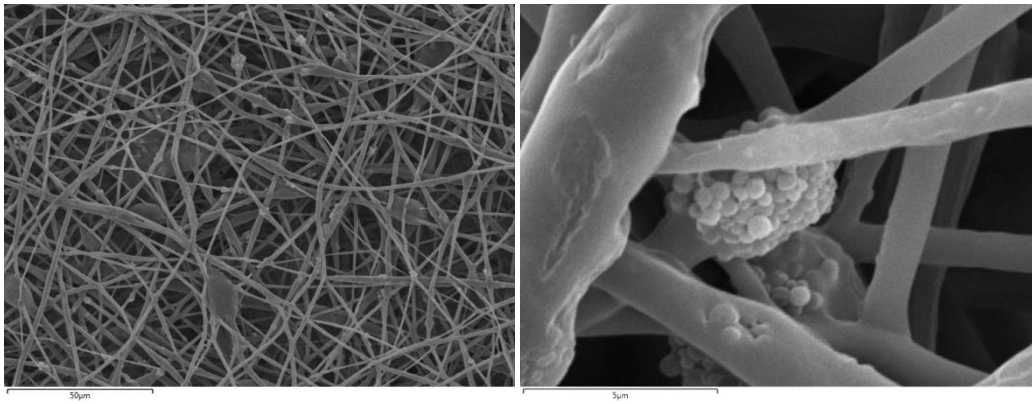

Figure 18 – SEM images for the membrane with 50%PLA content and addition of MSN's, after two weeks. Magnification: 750x(left), 10000x(right).

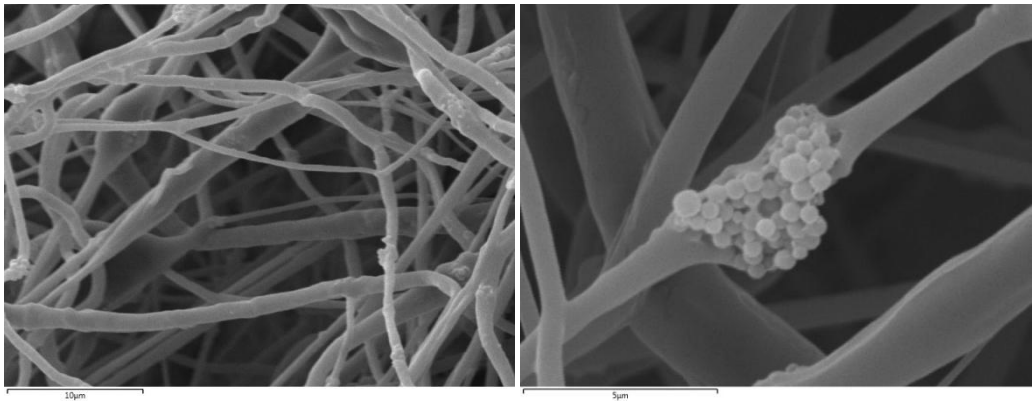

Figure 19 – SEM images for the membrane with 75%PLA content and addition of MSN's, after two weeks. Magnification: 750x(left), 10000x(right).

After two weeks it can easily be seen that the fibers have suffered degradation, however it is also clear that the amount of degradation for each membrane is different.

Starting with the membrane with 25% PLA content (figure 17), it is clear how much the fibers were affected. The first image on the left clearly shows missing segments on the fibers. These are likely to be the sites where there were previously MSN agglomerates, although they can also simply be broken fibers. On the image on the right, the fibers are clearly degraded and their structure has already begun breaking down. The second set of images (figure 18) shows that the 50% PLA content fibers did not suffer as much degradation as the previous ones, and although on the left missing segments on the fibers can be observed they occur much less, and on the right the fibers have not degraded as much and agglomerates of MSN's can still be seen. However if one looks closely these agglomerates show spots where MSN's were likely set. On the third and final membrane (Figure 19) the degradation is much less pronounced and the fibers themselves show very little signs of it, MSN agglomerates are still present as well although the loss of some particles is evident. On the last image on the right the missing MSN spots can be easily seen, and present an interesting detail to observe.

These differences in degradation of the fibers can be related to their composition. PLA and PLGA have different degradation times, with the latter degrading faster, and the mixture of these two polymers also affects the degradation rate of the fibers. This can be attributed to the lower hydrophobicity of PLGA [39].

4.4 Water contact angles

As described on the methods section, an analysis of the water contact angles was performed, in order to evaluate the level of hydrophobicity of the membranes' surface. The obtained results are represented in figure 21. Generally, if the water contact angle is larger than 90°, the surface can be considered hydrophobic and if the water contact angle is smaller than 90°, the surface is considered hydrophilic as can be observed on figure 20.

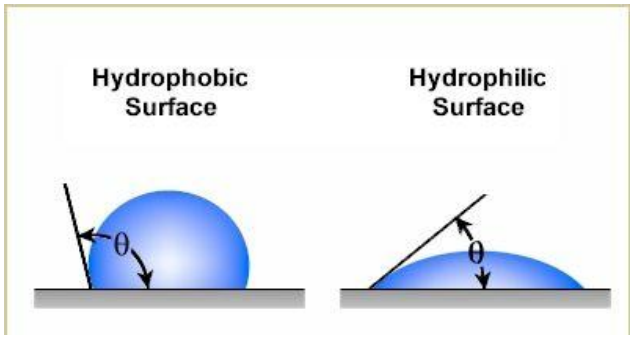

Figure 20 – Contact angles relation with hydrophobicity/hydrophilicity. Adapted from [40]

Due to the hydrophobic nature of the polymers used - PLA and PLGA- it was expected that the membranes without silica nanoparticles would exhibit a hydrophobic behavior. This supposition was confirmed by the obtained contacted angles that varied between 132 º and 137º. With the addition of silica nanoparticles, a hydrophilic material, the hydrophobicity of the membranes was liable to change. In fact, all membranes with silica had slightly inferior contact angles in comparison with the membranes with the same composition but without silica. Still, the contact angles values - that varied between 115º and 132º - indicate that the membranes with silica retain the hydrophobic character of the polymers. This can be justified by the small percentage of silica in the nanofibers (around 10% of the polymer weight) and by the fact that at least part of the nanoparticles are in the interior of the nanofibers.

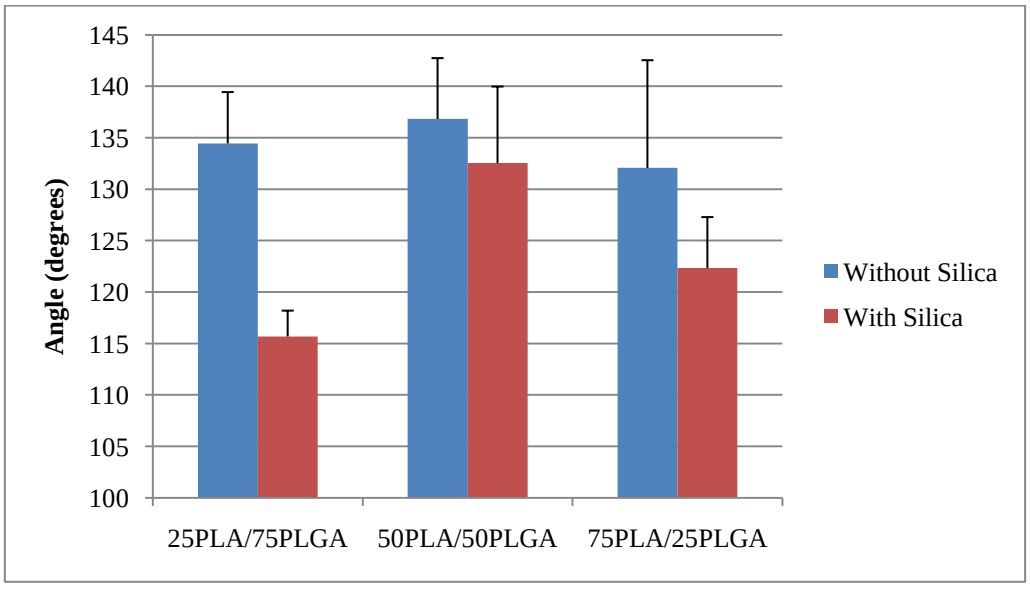

Figure 21 – Contact angles comparison for each polymer composition.

4.5 *In vitro* release

As stated on the methods section, *in vitro* release tests in PBS at 37ºC were performed for all the membranes in order to evaluate the GS release profiles. The results are presented here, split between membranes with GS dispersed in the polymer solution (Figure 22, Table 4), membranes with added npSi-GS (Figure23, Table 5), and finally the last batch of membranes with the hybrid load of GS in different quantities (Figure 24, Table 6).

Table 4 – Release data for the membranes without addition of MSN.

	Released % GS		
Time	**25PLA/75PLGA**	**50PLA/50PLGA**	**75PLA/25PLGA**
1h	7,3 ± 2,9	5,5 ± 0,8	8,3 ± 5,1
8h	34,0 ± 4,5	35,2 ± 2,1	39,4 ± 10,5
1 day	42,4 ±4,5	46,1 ± 8,2	48,0 ± 12,2
7 days	62,9 ± 8,2	71,7 ± 9,0	76,8 ± 6,0
14 days	74,2 ± 13,7	85,0 ± 7,9	89,4 ± 3,9
18 days	80,2 ± 14,4	93,2 ± 9,0	-

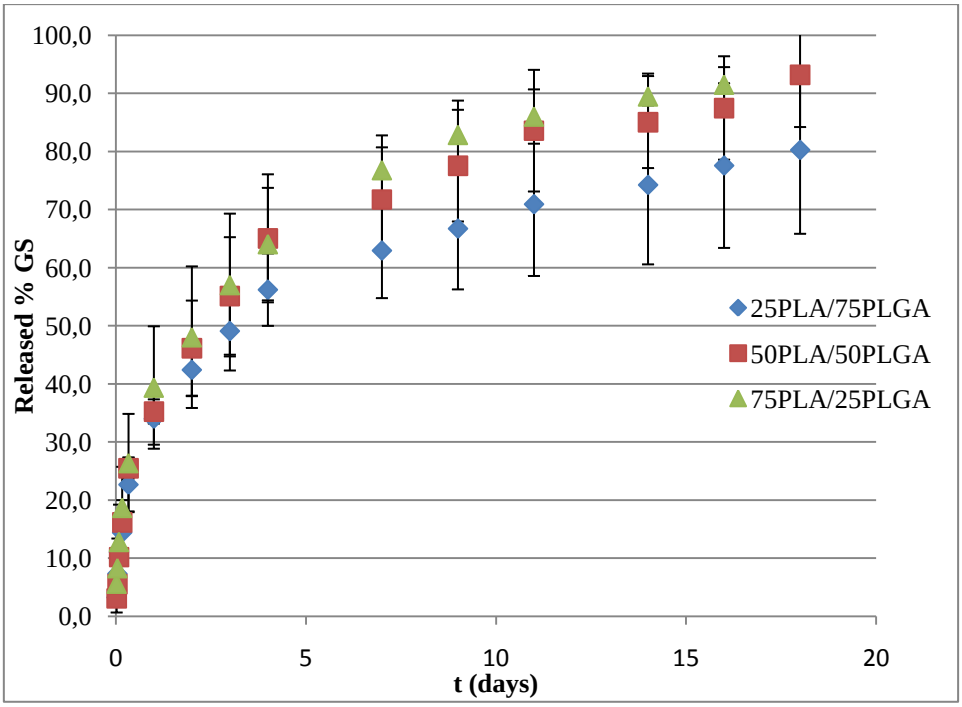

Figure 22 – Release profiles for the membranes without addition of MSN's.

The GS release profiles from the membranes without MSN's are very similar for all the three polymeric compositions. All membranes exhibit a burst release in the first day, with the release of around 40% of the antibiotic. After this first phase, the membranes exhibit a gradual release of the antibiotic until the end of the assay at the 18th day, when the percentage of GS release reaches a value equal or superior to 80%.

The GS release profiles from the membranes containing gentamicin loaded MSN's are presented in Figure 23 and Table 5. As it can clearly be observed, the addition of MSN's has resulted on a decrease of the release rate for all the membranes. This is especially pronounced for the one with equal quantities of both polymers, as the same polymer composition presented one of the higher release rates with no MSN addition, and with it presents the lowest with a drop of total GS released of over 50%. While the membrane with the least PLA (and the most PLGA) shows the least decrease of release rate, as well as released quantity, which is less than a 10% difference for the same polymer composition without silica.

Table 5 – Release data for the membranes with addition of MSN's.

	Released % GS		
Time	**25PLA/75PLGA**	**50PLA/50PLGA**	**75PLA/25PLGA**
1h	3,4	2,3	3,2
8h	29,0	12,9	14,3
1 day	37,7	15,4	17,5
7 days	51,9	23,0	28,8
14 days	60,3	31,0	43,5
18 days	71,6	39,4	53,1

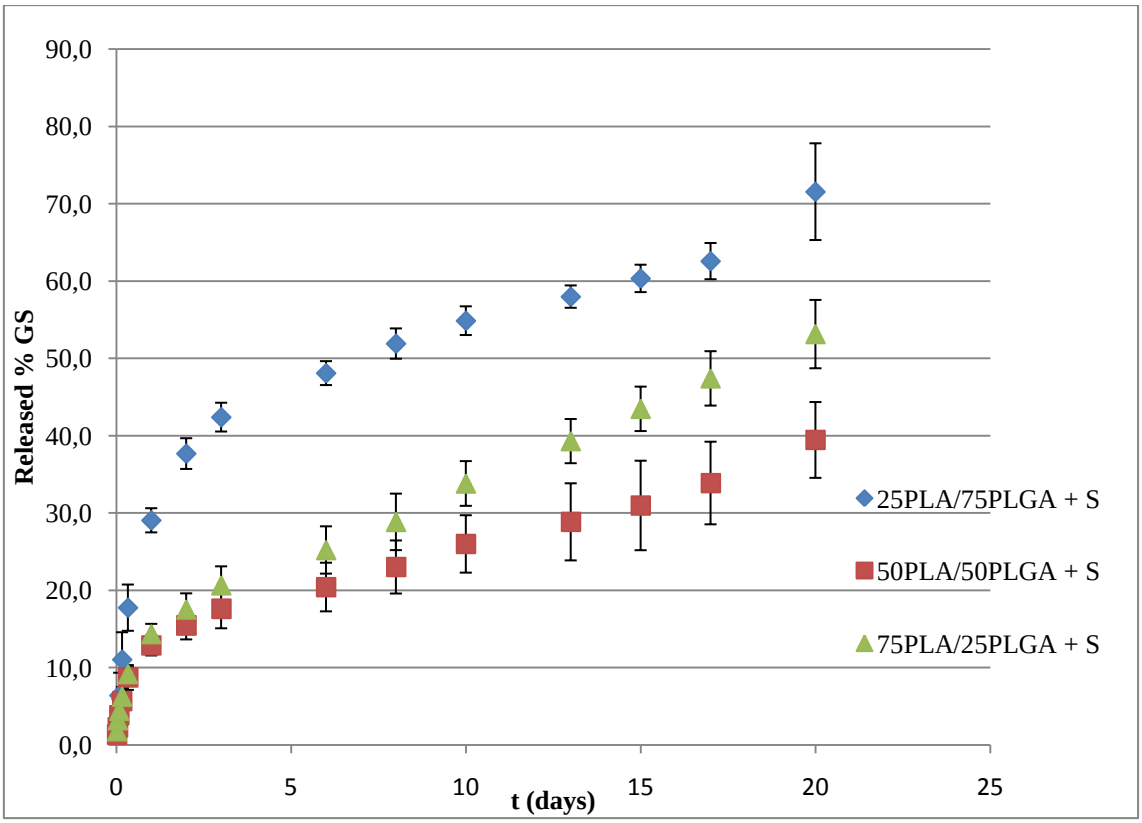

Figure 23 – Release profiles for the membranes with addition of MSN's.

Unlike with the membranes with no MSN addition, the release profiles are quite different among the polymer compositions. This can be related to the degradation rates analyzed before, since the membrane that shows the fastest release rate is also the one with the fastest degradation. This is to be expected since as the fibers start to degrade, the MSN's (loaded with GS) are released into the medium. At the same time, while the 50PLA/50PLGA fibers showed higher degradation than the 75PLA/25PLGA ones, they also show the slowest release rate. At first glance this might seem strange, however, upon observation of figures 18 and 19 it can be seen on figure 18 (50PLA/50PLGA) that while the fibers themselves are more degraded than the ones shown on figure 19 (75PLA/25PLGA), there are less MSN's missing from its agglomerates, while the opposite is apparently true for the 75PLA/25PLGA fibers.

In Figure 24 and Table 6 are the results for the GS release profiles of the hybrid load membranes. The graph clearly shows that the membrane with the highest quantity of GS (15%) has a very high initial release burst, where over 75% of the drug it contained was released after just one day, and over 92% after one week, leaving very little GS content in the membrane for the last week. This is, however, not unexpected

due to the quantity of GS present in these fibers. It is only natural that the higher concentration would result in a bigger initial burst and a faster release rate.

Table 6 – Release data for the membranes with hybrid load of GS.

	Released % GS	
Time	**5% GS**	**15% GS**
1h	-	8,1
8h	9,8	51,9
1 day	13,4	75,4
7 days	37,9	92,2
14 days	53,2	95,7
18 days	59,2	97,0

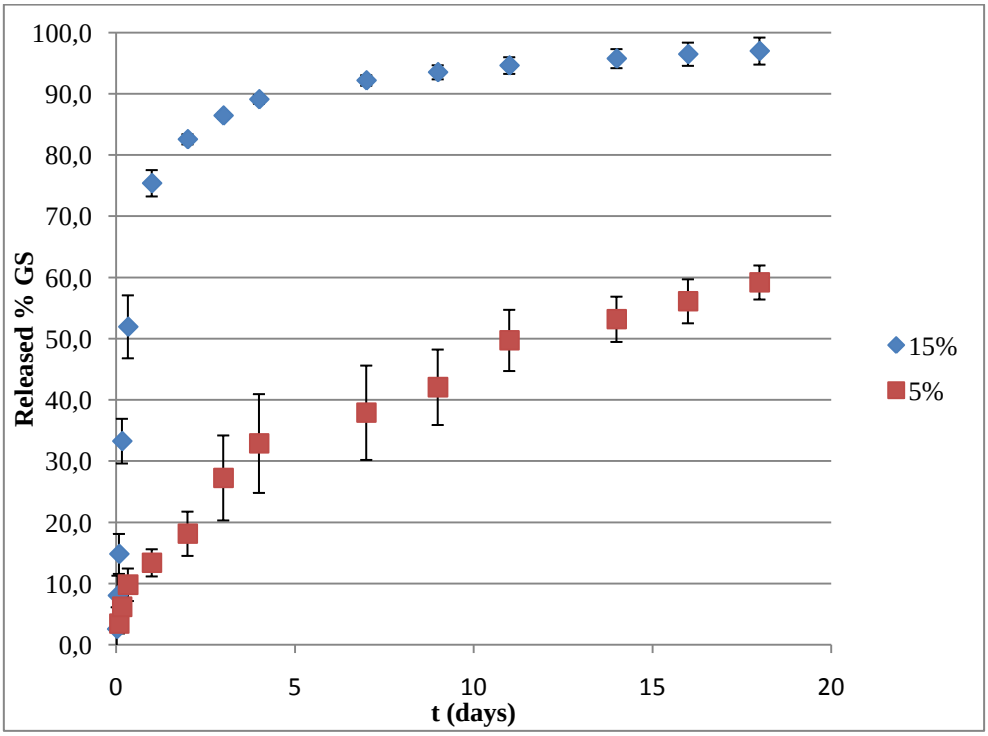

Figure 24 – Release profiles for the membranes with hybrid GS load.

Similarly expected is the much smaller initial burst of release for the membrane with the lowest quantity of GS, as well as a much slower release rate and a total release of GS fewer than 60%. However it is important to note the much more gradual release which becomes almost linear after three days. This almost linear behavior translates into a much more controlled release pattern, and could possibly mean that, given more time,

the membrane would have a much wider release window. It is regretful that the membrane with 10% GS load suffered contamination and therefore could not be included in the release tests, as it could, in principle, show a release profile that would fit between the ones presented in the graph, and could have very well presented the best solution for the three week window.

4.6 Antimicrobial activity

This section shows the results of the antimicrobial tests. As it was described on the methods section, 7mm discs were cut from all the samples. However the mass of each sample varied by a considerable margin, which is of course partly due to the different composition of the membranes, yet it must be noted that the membranes' density was not equal within all of its area, resulting in some parts being denser than others. Besides that factor, something that also affected the samples' final mass was the fact that some membranes, specifically the ones with higher quantity of PLGA, tended to stick to the tin foil they were deposited on and leave some material on it that was not possible to remove without destroying the membranes' structure.

The first results shown on table 7 and figure 25 refer to the control membrane. This membrane was a 50PLA/50PLGA membrane with no addition of GS in any form.

Table 7 – Results of the antimicrobial test for the control membranes.

Samples		**Mass (g)**	**Diameter of halo (cm)**
Control	**Sample 1**	3,28	0
	Sample 2	3,88	0

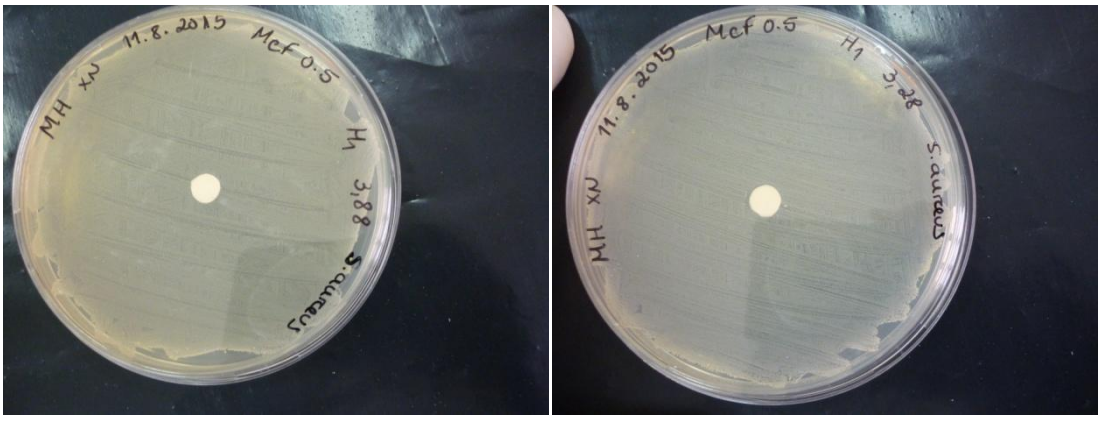

Figure 25 – Antimicrobial activity for the control samples.

Through observation of the images it is clear that the membranes themselves have no antimicrobial activity whatsoever, as expected, and therefore all the following results can be credited solely to the release of GS.

The results for the GS loaded membranes, without MSN addition are presented below on table 8, and figures 26 through 28.

Table 8 – Results of the antimicrobial test for the membranes with no MSN addition.

Samples		**Mass(g)**	**Diameter of halo (cm)**
25PLA/75PLGA	**Sample 1**	6,69	3,6-3,7
	Sample 2	6,50	3,6-3,7
50PLA/50PLGA	**Sample 1**	4,41	3,2
	Sample 2	4,95	3,2
75PLA/25PLGA	**Sample 1**	3,58	3,2
	Sample 2	3,72	3,2

As can be seen on the table above the sample masses vary considerably, the reasons for which were previously presented. This, in turn, has affected the quantity of GS released.

Figure 26 – Antimicrobial activity for the 25PLA/75PLGA samples.

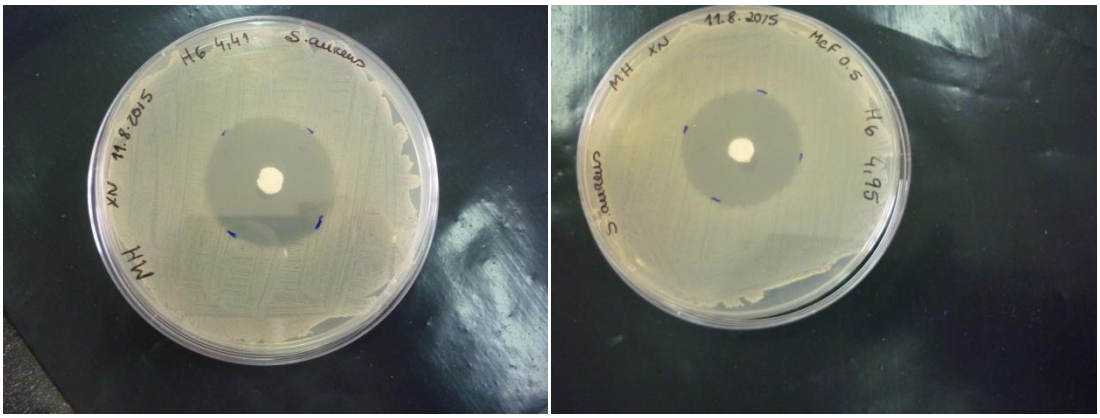

Figure 27 – Antimicrobial activity for the 50PLA/50PLGA samples.

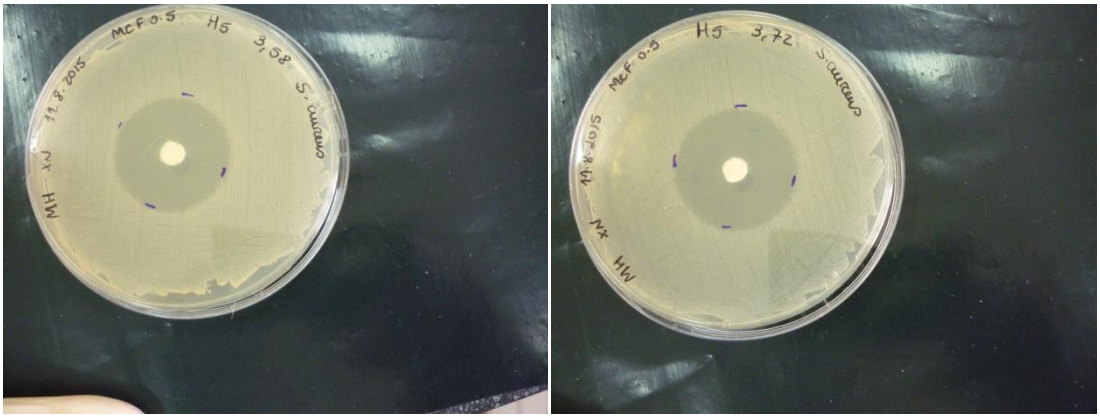

Figure 28 – Antimicrobial activity for the 75PLA/25PLGA samples.

From observation of the pictures the antibacterial effect can be seen on the bacterial population, which conclusively illustrates the presence of GS released by the membranes. The effect of the polymer composition on the release kinetics can also be observed to an extent, as the samples with the smallest mass, 75PLA/25PLGA, showed the same halo diameter as the 50PLA/50PLGA samples and close to the 25PLA/75PLGA samples, even with the steep difference in mass. This is also concordant with the *in vitro* release results shown before.

On table 9 the antibiotic results for the membranes with MSN addition are shown, the correspondent figures (29 through 31) are presented below the following table.

Table 9 – Results of the antimicrobial test for the membranes with MSN addition.

Samples		Mass (g)	Diameter of halo (cm)
25PLA/75PLGA with MSN's	**Sample 1**	6,14	3,2
	Sample 2	5,53	3,3
50PLA/50PLGA with MSN's	**Sample 1**	5,35	3,0
	Sample 2	5,43	3,0
75PLA/25PLGA with MSN's	**Sample 1**	7,32	3,2
	Sample 2	7,54	3,1

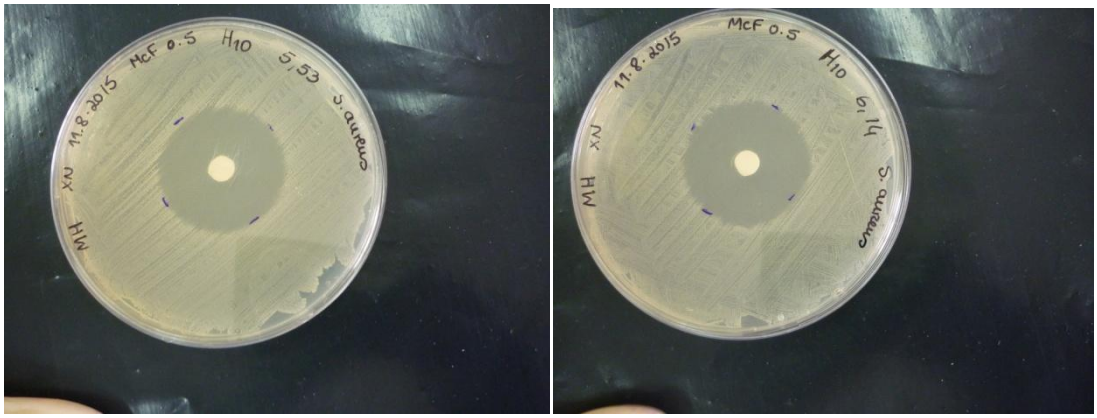

Figure 29 – Antimicrobial activity for the 25PLA/75PLGA samples with MSN's.

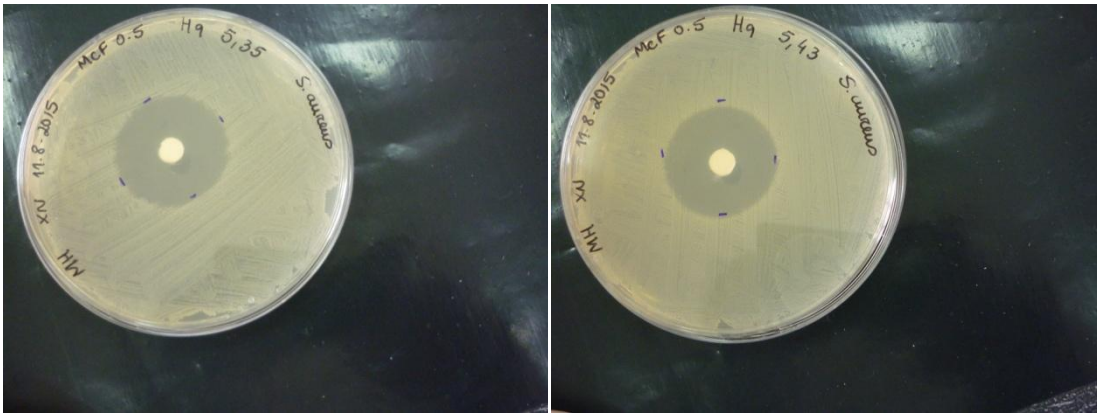

Figure 30 – Antimicrobial activity for the 50PLA/50PLGA samples with MSN's.

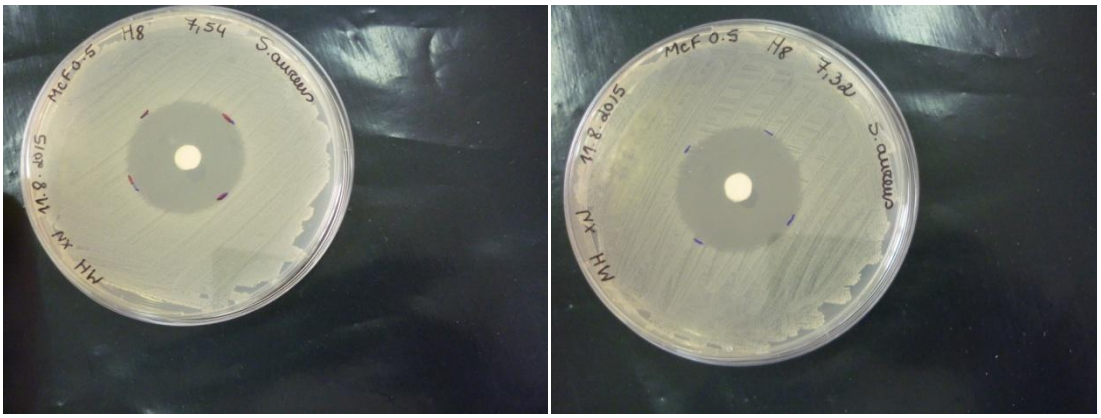

Figure 31 – Antimicrobial activity for the 75PLA/25PLGA samples with MSN's.

Similarly to what has been observed for the previous set of samples a defined halo was formed, evidencing the antibacterial effect of the membranes. However what is important to note in these results is the halo diameters these samples present which, despite the mass difference, are similar to the halo diameters of the previous samples. The conjunction of the larger mass with similar halo size indicate the slower release rate for these samples, thus supporting the *in vitro* release test results shown previously.

The hybrid load membranes were also tested for antibiotic activity. The results are shown on table 10 as well as figures 32 and 33, which are presented below.

Table 10 – Results of the antimicrobial test for the membranes with hybrid GS load.

Samples		**Mass (g)**	**Diameter of halo (cm)**
50PLA/50PLGA (5% GS content)	**Sample 1**	5,51	3,2
	Sample 2	5,55	3,3
50PLA/50PLGA (15% GS content)	**Sample 1**	3,74	3,5
	Sample 2	2,86	3,5

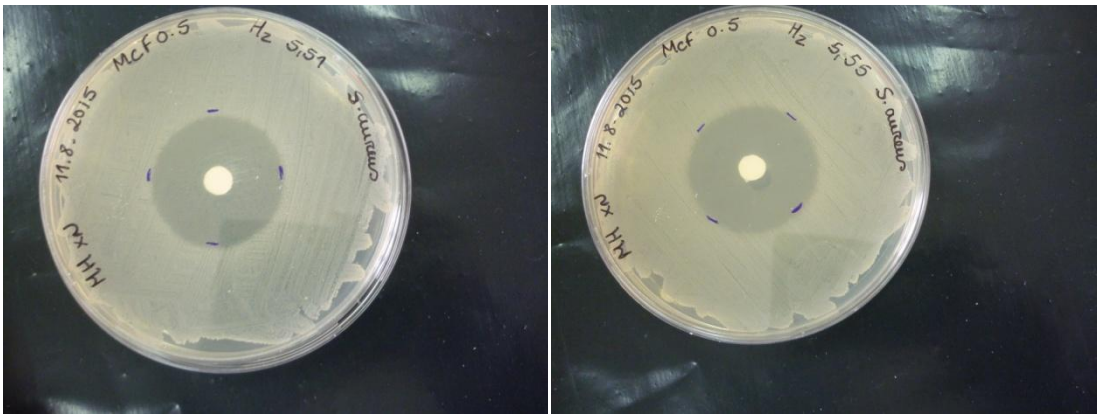

Figure 32 – Antimicrobial activity for the samples with 5% GS load.

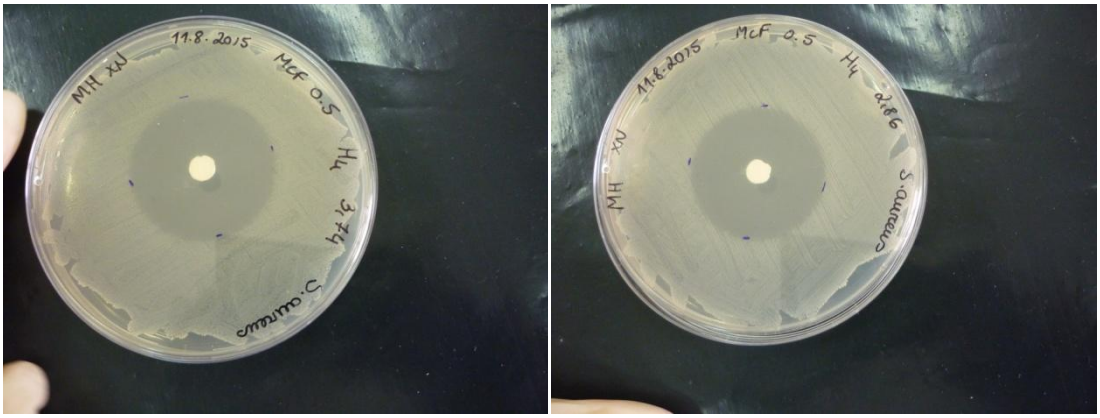

Figure 33 – Antimicrobial activity for the samples with 15% GS load.

As to be expected, the membrane with 15% GS content showed a large halo, the second largest in fact, even despite showing small mass values. This concurs with the data obtained before, as it was shown that this membrane presented a high initial release burst, and after one day over 75,4% of the GS content was released. The sample with 5% GS content showed similar results to the other MSN loaded samples, much like the *in vitro* release results for the same membrane.

To illustrate the effect of the contamination on the membrane with the 10% GS hybrid load, the antimicrobial test results were performed on it. The results are shown on table 11, and the pictures for them are shown on figure 34.

Table 11 – Results of the antimicrobial test for the membranes with hybrid GS load.

Samples		Mass (g)	Diameter of halo (cm)
50PLA/50PLGA (10% GS content)	**Sample 1**	7,00	0,0
	Sample 2	7,40	1,1

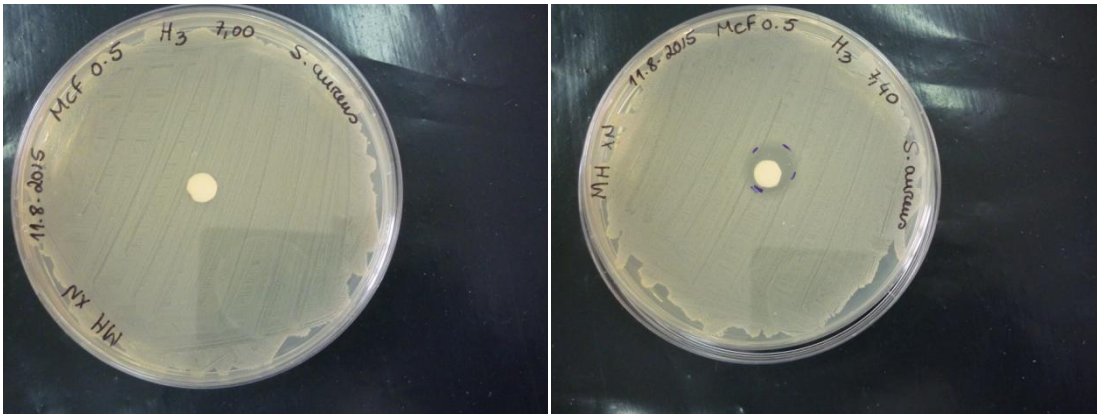

Figure 34 – Antimicrobial activity for the samples with 10% GS load.

As made abundantly clear by the results shown, the unknown contamination these samples suffered heavily impacted their drug release capabilities. The first sample shows no antimicrobial activity whatsoever, while the second sample shows a small amount of activity but well below all the previous samples, as well as what would be reasonably expectable considering its characteristics.

Chapter 5

Conclusions and Future Work

The GS was successfully loaded into three polymer mixtures of PLA and PLGA in different proportions, respectively 3:1, 1:1 and 1:3. The resulting electrospun membranes showed a good fibrous structure and a positive incorporation of the GS antibiotic. They also showed good drug delivery capabilities, having proven to have the ability to release drug in close to biological conditions (37ºC in PBS medium with 7,4pH). However this release was characterized by a sharp initial burst resulting in a very fast release of a high amount of drug. Almost 40% of the total drug was released during the first day and close to 80% after just 10 days.

GS was also successfully immobilized in mesoporous silica nanoparticles, which were subsequently mixed into three polymer mixtures of PLA and PLGA in the same proportions as the previous mentioned membranes. These membranes showed that the MSN's were well incorporated into the polymer fibers, which were able to hold them in agglomerates. These MSN loaded membranes showed a slower release rate, and were effective in reducing the initial burst that was present on the membranes without the MSN's. The release rates for these membranes were in general more controlled, resulting in much less GS quantity released over the same period of time (18 days). As low as 30% of total GS released was observed versus nearly 90% for the membranes lacking MSN's.

Polymer composition also played an important role on the release kinetics. While the differences were small for each polymer composition without MSN's, with their addition the difference in release rate for each polymer composition was evident. The 50PLA/50PLGA as well as the 75PLA/25PLGA membranes showed a marked drop of release rate with the addition of MSN's, while the 25PLA/75PLGA membrane showed very little difference. These results come from the different rates at which the membranes degrade in the medium. The latter membrane shows a much higher degree of degradation following three weeks of exposure to the medium, while the other membranes degrade at a noticeable slower rate, and while the 50PLA/50PLGA membrane is not the slowest to degrade it seems to be able to hold the MSN's for longer

when compared to the 75PLA/25PLGA membrane, which shows very little fiber degradation but a higher loss of MSN particles.

The hybrid loaded membranes also showed release profiles within the expected, where the membrane with the highest GS concentration showed the fastest release as well as a very sharp initial burst, having released over 90% of its total GS content after the 18 days period, while the 5% load membrane showed a much slower release rate with a much less pronounced release rate. The 10% membrane suffered contamination and therefore produced no results. From the observation of the release profiles of both valid hybrid membranes, it is not wrong to assume that the different loads can be used for different situations or even different stages of antibiotic therapy. While the initial burst of the 15% load membrane can be useful for early stages of therapy, the more controlled release of the 5% one may be more useful for later stages of the same therapy.

The antibacterial tests proved that the GS does not lose its antibiotic activity after being mixed with the polymers, being encapsulated in the MSN's and after going through electrospinning. When put in contact with the *Staphylococcus aureus* bacteria the membranes showed bactericidal capabilities after an exposure time of 24h, with halos forming around the round discs cut from the membranes in the bacterial population. Because the exposure time was just 24h the antibacterial halos showed similar diameter across all membranes, the only exceptions are for the 25PLA/75PLGA membrane with no MSN's and the 15% hybrid load membrane which showed halos notably larger than the others. However the higher antibacterial activity of the 25PLA/75PLGA membrane is attributed to its much larger mass and not from higher release capabilities, also supported by the release tests. The opposite is true for the 15% hybrid load, which had one of the lowest masses in the test and still came out with one of the biggest antibacterial halos observed.

Due to the marked difference in release rate between the hybrid load membranes, it would be worth manufacturing a second 10% hybrid load membrane as it would likely show an intermediate release pattern, and therefore possibly the best solution for the three week release period.

Owing to the results obtained for the nitrogen adsorption/desorption tests, it is safe to assume that a higher quantity of GS can be encapsulated into the MSN particles. This can be achieved by increasing the concentration of the drug in the impregnation solution, this being the most direct and obvious solution. However another way to

achieve a higher drug content in the MSN's is to control the pH levels, specifically, it has been proven that having the solution pH at 7, the drug loading can be substantially increased [41]. The increased quantity of GS into the MSN could potentially increase the release rate of the MSN loaded membranes, without reaching the rates seen on the membranes without silica or increase the release window length.

Another step to be taken is to develop strategies to counteract the MSN aggregation verified, thus obtaining a more uniform distribution of MSN particles throughout the fibers. In order to achieve this objective the surface of the MSN could be chemically modified to increase its hydrophobicity, thus increasing their affinity with the polymers in use.

References

[1] Charalampos G. Zalavras, Michael J. Patzakis, and Paul Holton, "Local Antibiotic Therapy in the Treatment of Open Fractures and Osteomyelitis," *Clinical Orthopaedics and Related Research*, no. 427, pp. 86-93, 2004.

[2] El-Refaie Kenawy et al., "Release of tetracycline hydrochloride from electrospun poly(ethylene-co-vinylacetate), poly(lactic acid), and a blend," *Journal of Controlled Release*, no. 81, pp. 57-64, 2002.

[3] Yuan Gao, Yen Bach Truong, Yonggang Zhu, and Ilias Louis Kyratzis, "Electrospun Antibacterial Nanofibers: Production, Activity, and In Vivo Applications," *Journal of Applied Polymer Science*, no. 131, 2014.

[4] Samit Kumar Nandi et al., "Local antibiotic delivery systems for the treatment of osteomyelitis - A Review," *Materials Science and engineering*, no. 8, pp. 2478-2485, 2009.

[5] Ijeoma F. Uchegbu, "Introduction," in *Polymers in Drug Delivery*, Taylor & Francis, Ed. Boca Raton, 2006.

[6] Sooyeon Kwon et al., "Silica-based mesoporous nanoparticles for controlled drug delivery," *Journal of Tissue Engineering*, vol. 4, 2013.

[7] Sungwon Kim, Jong-Ho Kim, Oju Jeon, Ick Chan Kwon, and Kinam Park, "Engineered Polymers for Advanced Drug Delivery," *European Journal of Pharmaceutics and Biopharmaceutics*, no. 3, pp. 420-430, 2009.

[8] Nano Pacific Holdings Inc. NanoPacific. [Online]. http://www.nanopacific.us/images/hard1.jpg

[9] M. Vallet-Regí, "Nanostructured mesoporous silica matrices in nanomedicine," *Journal of Internal Medicine*, no. 267, pp. 22-43, 2010.

[10] Igor I. Slowing, Vivero-Escoto Juan L, Chia-Wen Wu, and Victor S.-Y. Lin, "Mesoporous silica nanoparticles as controlled release drug delivery and gene transfection carriers," *Advanced Drug Delivery Reviews*, no. 11, pp. 1278-1288, 2008.

[11] Yu. A. Shchipunov, Yu. V. Burtseva, T. Yu. Karpenko, N. M. Schevchenko, and T. N. Zvyagintseva, "Highly efficient immobilization of endo-1,3-beta-D-glucanases (laminarases) from marine mollusks in novel hybrid olysaccharide-silia

nanocomposites with regulated composition," *Journal of Molecular Catalysis B Enzymatic*, vol. 40, no. 1, pp. 16-23, 2006.

[12] Igor I. Slowing, Brian G. Trewyn, Supratim Giri, and Victor S.-Y. Lin, "Mesoporous Silica Nanoparticles for Drug Delivery and Biosensing Applications," *Advanced Functional Materials*, vol. 17, no. 8, pp. 1225-1236, 2007.

[13] M. Manzano et al., "Studies on MCM-41 mesoporous silica for drug delivery: Effect of particle morphology and amine functionalization," *Chemical Engineering Journal*, vol. 137, no. 1, pp. 30-37, 2007.

[14] Lei Yang, Brian W. Sheldon, and Thomas J. Webster, "Nanophase Ceramics for Improved Drug Delivery: Current Opportunities and Challenges," *American Ceramic Society Bulletin*, vol. 89, no. 2, pp. 24-32, 2010.

[15] Luke Burke, Amir Keshavri, Nidal Hilal, and Chris J. Wright, "Electrospinning A Practical Approach for Membrane Fabrication," in *Membrane Fabrication*, Taylor & Francis, Ed. Boca Raton, 2015, ch. 2, pp. 45-47.

[16] Nick Tucker, Jonathan J. Stranger, Mark P. Staiger, Hussam Razzaq, and Kathleen Hofman, "The History of the Science and Technology of Electrospinning from 1600 to 1995," *Journal of Engineered Fibers and Fabrics*, no. Special Issue, pp. 63-73, 2012.

[17] Dan Li and Younan Xia, "Electrospinning of Nanofibers: Reiventing the Wheel?," *Advanced Materials*, vol. 16, no. 14, pp. 1151-1170, 2004.

[18] Dapeng Li, Margaret W. Frey, and Antje J. Baeumner, "Electrospun acid nanofiber membranes as substrates for biosendor assemblies," *Journal of Membrane Science*, vol. 279, no. 1-2, pp. 354-363, 2006.

[19] Darrell H. Reneker and Alexander L. Yarin, "Electrospinning jets and polymer nanofibers," *Polymer*, vol. 49, no. 10, pp. 2387-2425, 2008.

[20] A. L. Yarin, S. Koombhongse, and Darrell H. Reneker, "Taylor cone and jetting from liquid droplets in electrospinning of nanofibers," *Journal of Applied Physics*, vol. 90, no. 9, pp. 4836-4846, 2001.

[21] Robert Lamberts. (2008) Wikipedia. [Online]. https://upload.wikimedia.org/wikipedia/commons/6/6e/Taylor_cone_photo.jpg

[22] Dan Li and Younan Xia, "Fabrication of Titania Nanofibers by Electrospinning,"

Nano Letters, vol. 4, no. 4, pp. 555-560, 2003.

[23] Xiuli Hu et al., "Electrospinning of polymeric nanofibers for drug delivery applications," *Journal of Controlled Release*, vol. 185, pp. 12-21, 2014.

[24] Viness Pillay et al., "A Review of the Effect of Processing Variables on the Fabrication of Electrospun Nanofibers for Drug Delivery Applicaions," *Journal of Nanomaterials*, vol. 2013, 2013.

[25] Jianshe Huang and Tianyan You, "General Process of Electrospinning," in *Electrospun Nanofibers: From Rational Design, Fabrication to Electrochemical Sensing Applications*, Russel Maguire, Ed., 2013, ch. 2.

[26] Bochu Wang, Yazhou Wang, Tieying Yin, and Qingsong Yu, "Applications of Electrospinning in Drug Delivery," *Chemical Engineering Communications*, vol. 197, no. 10, pp. 1315-1338, 2010.

[27] Poonsub Threepopnatkul et al., "Mechanical and Antibacterial Properties of Electrospun PLA/PEG Mats," *Journal of Metals, Materials and Minerals*, vol. 20, no. 3, pp. 185-187, 2010.

[28] Kexin Qiu et al., "Doxorubicin-loaded electrospun poly(L-lactic acid)/mesoporous silica nanoparticles composite nanofibers for potential postsurgical cancer treatment," *Journal of Materials Chemistry B*, vol. 1, no. 36, pp. 4601-4611, 2013.

[29] Xuetao Shi et al., "Novel mesoporous silica-based antibiotic releasing scaffold for bone repair," *Acta Biomaterialia*, vol. 5, no. 5, pp. 1697-1707, 2009.

[30] Botao Song, Chengtie Wu, and Jiang Chang, "Controllable delivery of hydrophilic and hydrophobic drugs from electrospun poly(lactic-co-glycolic acid)/mesoporous silica nanoparticles composite mats," *Journal of Biomedical Materials Research Part B Applied Biomaterials*, vol. 100, no. 8, pp. 2178-2186, 2012.

[31] Jaspaul S. Gogia, John P.Meehan, Paul E. Di Cesare, and Jamali Amir A, "Local Antibiotic Therapy in Ostheomyelitis," *Seminars in Plastic Surgery*, vol. 23, no. 2, pp. 100-107, 2009.

[32] Alex C. McLaren, "Alternative Materials to Acryic Bone Cement for Delivery of Depot Antibiotics in Orthopaedic Infections," *Clinical Orthopaedics and Related Research*, vol. 427, pp. 101-106, 2004.

[33] Shou-Cang Shen et al., "Mesoporous silica nanoparticle-functionalized poly(methyl metacrylate)-based bone cement for effective antibiotics delivery,"

Journal of Materials Science: Materials in Medicine, vol. 22, no. 10, pp. 2283-2292, 2011.

[34] R.Srikar, A. L. Yarin, C. M. Megaridis, A. V. Bazilevsky, and E. Kelley, "Desorption-Limited Mechanism of Release from Polymer Nanofibers," *Langmuir*, vol. 24, no. 3, pp. 965-974, 2008.

[35] Pattama Taepaiboon, Uracha Rungsardthong, and Pitt Supaphol, "Drug-loaded electrospun mats of poly(vinyl alcohol) fibres and their release characteristics of four model drugs," *Nanotechnology*, vol. 17, no. 9, pp. 2317-2329, 2006.

[36] Botao Song, Chengtie Wu, and Jiang Chang, "Dual drug release from electrospun poly(lactic-co-glycolic acid)/mesoporous silica nanoparticles composite mats with distinct release profiles," *Acta Biomaterialia*, vol. 8, no. 5, pp. 1901-1907, 2012.

[37] K. Bajer, R. Malinowsky, D. Bajer, and S. Richert, "Properties of poly(lactic acid)/Ecoflex rigid foil sheets applied in thermoforming process," *Polimery*, vol. 55, no. 7-8, pp. 591-593, 2010.

[38] P. Frutos Cabanillas, E. Díez Peña, J. M. Barrales-Rienda, and G. Frutos, "Validation and in vitro characterization of antibiotic-loaded bone cement release," *International Journal of Pharmaceuticals*, vol. 209, no. 1-2, pp. 15-26, 2000.

[39] Catherine Shasteen and Young Bin Choy, "Controlling Degradation Rate of Poly(lactic acid) for Its Biomedical Applications," *Biomedical Engineering Letters*, vol. 1, no. 3, pp. 163-167, 2011.

[40] Ramé-Hart. ramé-hart Contact Angle. [Online]. http://www.ramehart.com/contactangle.htm

[41] A. L. Doadrio et al., "Mesoporous SBA-15 HPLC evaluation for controlled gentamicin drug delivery," *Journal of Controlled Release*, vol. 97, no. 1, pp. 127-132, 2004.

Annex A

Sample	%mass lost (pm)	%mass remaining (mr)
np-Si	~0	~100
GS	74,8	25,2
npSi-GS	22,0	78,0

Remaining mass of silica nanoparticles in function of initial silica mass:

$$mr(np\text{-}Si) = 1 * m(np\text{-}Si)$$

Remaining GS mass in function of initial GS mass:

$$mrGS = 0{,}252 * mGS$$

Considering 100g of npSi-GS:

$m(npSi\text{-}GS) = mGS + m(npSi) = 100 \rightarrow m(np\text{-}Si) = 100 - mGS$

Remaining mass in the GS loaded MSN's:

$mr(npSi\text{-}GS) = mrGS + m(npSi)$

$78 = 0{,}252mGS + (100 - mGS)$

$78 - 100 = 0{,}252mGS - mGS$

$mGS = 29{,}4\ g$

%GS loading in MSN's:

$\%(mGS/m(npSi\text{-}GS)) * 100 = (29{,}4/100) * 100 \approx \mathbf{30\%}$